EUROPEAN ORGANIZATION FOR NUCLEAR RESEARCH

NP Internal Report 73-5
12 April 1973

ISR RESULTS ON PROTON-PROTON ELASTIC SCATTERING AND TOTAL CROSS-SECTIONS

Ugo Amaldi*)

Physics Laboratory, Istituto Superiore di Sanità
and Istituto Nazionale di Fisica Nucleare, Sezione Sanità, Roma

CONTENTS

To be published in "Highlights in particle physics",
editor A. Zichichi, publisher Editrice Compositori, Bologna, Italy

---

*) At present CERN Visiting Scientist.

1. INTRODUCTION

In two years of running at the CERN Intersecting Storage Rings (ISR) two groups have collected a large amount of data on very high energy proton-proton elastic scattering. The Aachen-CERN-Harvard-Genova-Torino Collaboration (ACHGT) has used magnetostrictive spark chambers to detect the two protons elastically scattered at angles larger than about 10 mrad, while in our experiment (CERN-Rome Collaboration) the protons were detected by hodoscopes placed very close to the stored beams ($\geq$ 2 mrad). In the early stages of both experiments the minimum angles were about 5 mrad larger than the quoted values.

With an apparatus mounted in a different intersection region, the Pisa-Stony Brook Collaboration has collected data on the beam-beam total interaction rate with a counter system, and has thus measured the proton-proton cross-section.

The purpose of the present paper is to summarize the status of our knowledge concerning elastic scattering and total cross-sections and to present preliminary results of the work under way.

2. FORWARD NUCLEAR ELASTIC SCATTERING ($0.03 \leq |t| \leq 0.3$ GeV^2)

The results, published already in 1971 by the ACHGT and the CERN-Rome Collaborations[1,2,3], refer to the logarithmic slope b of the differential cross-section measured in different t ranges at various momenta of the colliding beams and are summarized in Table 1.

The slope b is obtained by fitting the unnormalized differential cross-section, measured in the t-intervals indicated in the table, with an exponential behaviour:

$$\frac{d\sigma}{dt} = A\, e^{bt} \quad . \tag{1}$$

The difference between the b values obtained in the two experiments clearly showed that a single exponential cannot fit the data in the range $0.03 \leq |t| \leq 0.3$ GeV^2. Indeed a non-exponential behaviour in this

Table 1

Slope b of the forward differential cross-section

ISR momenta (GeV/c)	s (GeV^2)	range of $\|t\|$ (GeV^2)	b (GeV^{-2})	Ref.
15.5 + 15.5	950	0.015 - 0.055	13.0 ± 0.7	3
		0.06 - 0.18	12.0 ± 0.2	2
22.5 + 22.5	2000	0.03 - 0.12	12.9 ± 0.4	3
		0.11 - 0.34	11.1 ± 0.15	2
26.5 + 26.5	2780	0.04 - 0.16	13.0 ± 0.3	3
		0.16 - 0.45	10.9 ± 0.15	2

Table 2

Slope b of the differential cross-section obtained by the ACHGT Collaboration[5]

ISR momenta (GeV/c)	Equivalent laboratory momentum (GeV/c)	s (GeV^2)	range of $\|t\|$ (GeV^2)	b (GeV^{-2})
10.8 + 10.8	245	460	0.050 - 0.094	11.57 ± 0.3
			0.138 - 0.238	10.42 ± 0.17
15.5 + 15.5	505	950	0.046 - 0.090	11.87 ± 0.28
			0.138 - 0.240	10.91 ± 0.22
22.5 + 22.5	1070	2000	0.046 - 0.089	12.87 ± 0.20
			0.136 - 0.239	10.83 ± 0.20
26.5 + 26.5	1480	2780	0.060 - 0.112	12.40 ± 0.30
			0.168 - 0.308	10.80 ± 0.20

range had already been suggested by a compilation of data obtained at conventional accelerators[4].

Recently the ACHGT Collaboration has published the results of a new experiment which covers a wider t range at four different energies[5]. The angular distributions (one of them appears in Fig. 1) confirm the fact that the slope of the differential cross-section changes around $|t| \simeq 0.1$ GeV . The values of the slope obtained in this experiment are collected in Table 2.

More recently the CERN-Rome Collaboration has remeasured, with the apparatus described below, the slope at even smaller momentum transfers[6]. The data are collected in Table 3.

Table 3

Slope b obtained by the CERN-Rome Collaboration[6,37]

ISR momenta (GeV/c)	Equivalent laboratory momentum (GeV/c)	range of $\|t\|$ (GeV^2)	b (GeV^{-2})
22.6 + 22.6	1070	0.01 - 0.05	12.6 ± 0.4
26.6 + 26.6	1480	0.01 - 0.06	13.1 ± 0.3
31.4 + 31.4	2070	0.01 - 0.06	13.1 ± 1.0

These data, together with the results summarized in Table 1, show that, at least at 22.5 and 26.5 GeV, the slope does not vary when the average momentum transfer decreases from $|t| \simeq 0.08$ GeV^2 to $|t| \simeq 0.03$ GeV^2. The average values derived from the measurements of the CERN-Rome Collaboration are:

$$s = 2000\ GeV^2; \quad 0.01 < |t| < 0.12 \quad b = (12.8 \pm 0.3)\ GeV^{-2}$$
$$s = 2800\ GeV^2; \quad 0.01 < |t| < 0.16 \quad b = (13.1 \pm 0.2)\ GeV^{-2} .$$

The previous values at small momentum transfers, and the results obtained at other accelerators, are plotted versus s in Fig. 2. From the figures and the tables the following conclusions can be drawn. There exist two t-regions where the data are reasonably well represented by exponentials and the change of slope occurs smoothly around $|t| \simeq 0.1$ GeV^2. However, other parametrizations are certainly possible. All the data at $|t| \lesssim 0.15$ GeV can be fitted[5] with a simple logarithmic dependence upon s:

$$b = \tilde{b} + 2\alpha' \ln s \qquad (2)$$

if the Serpukhov data[7] are lowered by $\Delta b = 0.4$ GeV^2, which is 1.3 times the quoted systematic uncertainty in the b scale. The fitted parameters are $\tilde{b} = (7.0 \pm 1.1)$ GeV^{-2} and $\alpha' = (0.37 \pm 0.08)$ GeV^{-2}. Let us recall that the Serpukhov data alone give $\alpha' = (0.47 \pm 0.09)$ GeV^{-2} [7].

A parametrization similar to Eq. (2) is also possible for the large momentum transfer region, where the parameter α' appears to be smaller ($\alpha \simeq 0.1$ GeV^{-2}).

If the Serpukhov data are lowered by $\Delta b = 0.4$ GeV^2, one reaches the conclusion that the logarithmic shrinkage of the very forward diffraction peak continues up to ISR energies (i.e. up to $\sim$ 1500 GeV/c equivalent laboratory momentum). On the other hand if the Serpukhov data are not lowered (as in Fig. 2), one is tempted to conclude that the shrinking of the forward peak continues, but less rapidly than suggested by an extrapolation of the lower energy data. In conclusion one cannot definitely state that the simple parametrization of Eq. (2) represents the data at small momentum transfers and if one intends to obtain a definite answer for the detailed dependence of b upon s it is necessary to reduce the systematic errors in the measurement of the forward slope to ~ 0.1 GeV^{-2} at all energies.

The new ISR data have proved that the logarithmic slope of the differential cross-section is a function of the momentum transfer and many models have been proposed to explain this effect. To get a feeling of the physical meaning of the change of slope with the momentum transfer, we write down two possible rough representations of the ISR data in terms of the sum of two exponentials:

$$\frac{d\sigma}{dt} = A_1 \left(e^{-11|t|} + 0.37\, e^{-34|t|}\right) \quad \text{(incoherent sum)}$$
$$\frac{d\sigma}{dt} = A_2 \left(e^{-5|t|} + 0.27\, e^{-18|t|}\right)^2 \quad \text{(coherent sum)} \; . \tag{3}$$

By recalling that in an optical model with constant opacity, the radius R of the interaction determines the slope parameter b:

$$b = \frac{R^2}{4} \; , \tag{4}$$

the simple fits of Eq. (3) indicate that the interacting protons feel two regions, whose radii are $\sim$ 1.3 fm ($b \simeq 11$ GeV^2) and $\sim$ 2.3 fm ($b \simeq 35$ GeV^2). Of course this is too simple an interpretation, but in various models which have been proposed the scattering amplitude is indeed written as the sum of at least two contributions which have different t-dependences, i.e. which differ in their space behaviour. In other models the change of slope is due to multiple scattering effects, as will be seen in the following.

The models proposed to explain the behaviour of the differential cross-section can be subdivided into two classes according to the role played by the real part of the nuclear amplitude. In the first class the amplitude is either imaginary (as in Eq. (3)) or with a small real part, whilst in the second class the real part is essential in determining the angular dependence of the differential cross-section.

To the first class belong the models proposed by Edelstein[8], Carreras and White[9], White[10], Heckman and Henzi[11], Barshay[12], and various types of Regge models.

Edelstein[8] considers the elastic scattering of physical protons as a regenerative process due to the fact that the proton is a composite system $|N\rangle$ of two eigenstates $|a\rangle$ and $|b\rangle$, each of which has its own vertex function exponential in t. Then one can write

$$|N\rangle = \cos\phi\, |a\rangle + \sin\phi\, |b\rangle$$

and the four amplitudes of Fig. 3a contribute to the scattering of two physical protons. The ortagonal combination of the states $|a\rangle$ and $|b\rangle$ has the same quantum numbers as the nucleon and is identified with the physical $N^*(1400)$:

$$|N^*\rangle = - \sin \phi \, |a\rangle + \cos \phi \, |b\rangle \ .$$

The graphs of Fig. 3b contribute to the diffraction dissociation of the nucleon in $N^* + N$ (graphs in which N and N^* are exchanged in the final state are left out for simplicity). The vertex functions (which are supposed to follow factorization) are written in the form

$$\beta = \beta_0 \, e^{\lambda t} \ , \quad \gamma = \gamma_0 \, e^{\mu t} \ ,$$

so that, together with the phase ϕ, the model contains five parameters which can ve determined at 30 GeV/c of laboratory momentum from experimental data on elastic scattering and $N^*(1400)$ production. The predicted N^* slope is then 23 GeV^{-2}, in good agreement with the experiment. The model predicts also a minimum in the N^* angular distribution at 0.25 GeV^2. An indication of a minimum around 0.3-0.4 GeV has been obtained by the CERN-Rome Collaboration at 24 GeV/c [13]. This model cannot be tested at ISR energies because N^* cross-sections are still lacking, but it has the advantage of connecting two different processes through a natural generalization of a well-known mechanism: diffraction dissociation. Since the same mechanism is effective in all channels, one expects a complex t dependence of all elastic scattering data, in agreement with recent observations.

Carreras and White [9] extend the optical model of Chou-Yang [14], which considers asymptotic diffraction scattering as due to the strong local absorption of the incident waves. This absorption is taken to be proportional to the overlap of the two extended distributions of hadronic matter $\rho(r)$, which in turn are supposed to be proportional to the charge densities of the interacting protons. With this hypothesis the Chou-Yang phase-shift is a function of the impact parameter a:

$$\delta(a) \propto i \int \rho(\vec{r}_1)\rho(\vec{r}_2)\delta(\vec{a} - \vec{x}_1 - \vec{x}_2)d^3\vec{r}_1\, d^3\vec{r}_2 \qquad (5)$$

(the bi-vector $\vec{x}_i$ is the position of a small volume of the interacting particle i in a plane perpendicular to the velocity). Carreras and White substitute to the contact interaction factor $\delta(\vec{a} - \vec{x}_1 - \vec{x}_2)$ an extended interaction (which reduces to a δ-function at infinite energy) and assume the usual dipole form for the Fourier transform of the density $\rho(\vec{r})$. The model contains two parameters, one specifying the degree of non-locality and the second the behaviour of the non-locality with energy. The computed values of the logarithmic slope for different momentum transfer agree reasonably well with the experimental data. An extension of the Chou-Yang model has also been used by Lo and Thomson to compute the forward slope[15].

White[10] remarks that the original Chou and Yang model with a contact interaction fits the measured behaviour of the differential cross-section if a dipole formula $\left[1 - t/\mu^2\right]^{-2}$ is assumed for the "matter form factor". The best fitted μ^2 is found to vary in the ISR energy range by about 7% around the value $\mu^2 = 0.71$ GeV^2 obtained in fitting the charge form factor measured in electron scattering. This connection is clearly very appealing and the fits are also very good, as it appears from Fig. 4. It must be noted that this model (as well as all others) does not reproduce the deviations of the experimental points from a smooth line, which are very apparent in the representation of Fig. 4. Since these deviations are small, more experimental work is needed before one can be sure of their absolute value and position.

Heckman and Henzi[11] point out that the upward concavity of the angular distribution has a simple explanation in terms of the overlap function approach first introduced by Van Hove[16], where the contributions of many-body states to the two-body unitarity relation are lumped together and expressed as a simple exponential in t. Such an overlap function is consistent with the exchange of a Pomeron trajectory having a slope around t = 0 of the order of 0.2 GeV^{-2}.

Barshay[12] connects the t-dependence of the slope to the behaviour of the inelastic amplitudes, which produce diffraction scattering through

their shadow. He writes the nearly energy-independent total inelastic cross-section in the form $\Sigma_n \sigma_n$ (where σ_n is the n-particle production cross-section) and introduces the hypothesis that two different mechanisms contribute to each σ_n. The first mechanism involves no exchange of quantum numbers and gives rise to a σ_n which is energy-independent, while the other is not vacuum-exchange and produces inelastic cross-sections which decrease with energy but sum up to a finite contribution in the total inelastic cross-section. The t-dependencies of these two processes are different so that their shadow has a complex t-behaviour. The model is not quantitative and the t-dependence of the two inelastic contributions has to be guessed, applying some Regge recipe to the two-cluster model; but it has the interesting feature of proposing a common mechanism for the slope variation in proton-proton scattering and for the decrease of the very forward slope in the reaction

$$p + p \to X + p \ ,$$

when the mass of the produced cluster X increases. This effect is observed at incident laboratory momenta smaller than 30 GeV/c.

Many Regge-pole models have been proposed to fit the forward proton-proton slope, as measured at the ISR, together with lower energy data. Since a complete review of these models is beyond the scope of the present contribution, we shall consider only some of the many published papers.

Austin and Rarita[17] conclude, from a four-pole fit to high-energy pp and $\bar{p}p$ elastic scattering, that the t-dependence of the slope parameter b is a reflection of the non-zero slope of the Pomeranchuk trajectory. Barger, Geer and Phillips[18] discuss various possible combinations of a flat (or a sloping) Pomeranchuk trajectory with secondary Regge contributions and with cuts. They conclude that the data admit several different explanations. Pomeron slopes in the range 0-0.4 GeV^{-2} have been obtained in other models[19].

Barnett[20] has used the model proposed by Arnold and Barnett which contains a fixed Pomeron pole (i.e. a Pomeranchuk trajectory of zero slope) plus a cut which is chosen in such a way as to avoid violations of t-channel unitarity and gives a negative contribution to the total

cross-section. For this reason the model predicts a proton-proton cross-section which rises appreciably with energy.

Barger, Phillips and Geer[21] consider the contributions to proton-proton and antiproton-proton elastic scattering due to Pomeron-, f- and ω-exchanges, and find that good fits to the ISR data can be obtained by writing the Pomeron-exchange amplitude as the sum of two contributions. The first contribution is exponential in t with a slope of about 4 GeV^{-2}, while the second contribution is peripheral and has the form

$$A_{periph} \sim e^{b't} J_0(R\sqrt{|t|}) \tag{6}$$

with a radius $R \simeq 1$ fm (the exponential factor comes from the fact that the edge of radius R is spread). The authors judge this hypothesis to be physically more appealing than the exponentially peripheral term of big slope appearing in Eq. (3). By fitting the data from 20 GeV to ISR energy, they find ~ 0.2 GeV^{-2} for the slope of the Pomeron trajectory.

As a conclusion of this short description of various Regge models, one can say that in spite of the fact that Eq. (2) represents reasonably well the energy dependence of the slope of the forward proton-proton cross-section, no definite conclusion can be drawn regarding the nature of the Pomeron trajectory. This fact shows that these models are too flexible, more than indicating that extension of the data at higher energies and measurement of the other physical quantities are needed.

Passing now to the class of models in which the real part plays an important role, we briefly consider Kane ansatz[22]. Kane writes the proton-proton amplitude as

$$A = A_{disc} + A_{edge} = C\, e^{bt} + \mathrm{Im}\, A_{edge} + \mathrm{Re}\, A_{edge} \,. \tag{7}$$

As in Ref. 21, for $\mathrm{Im}\, A_{edge}$ the form of Eq. (6) is assumed, but a real part is added, which vanishes in the forward direction but otherwise is significantly different from zero.

The introduction of a sizeable real nuclear amplitude in this and other models of the same class does not seem sufficiently justified at this stage. We conclude this presentation by summarizing the two main

points of view introduced in the models described above, which try to justify the t-dependence of the proton-proton slope parameter. In one approach the effect is produced in a very natural way by treating the protons as absorbing disks, as suggested by Chou and Yang. In the second approach the change of slope is the reflection of the presence of amplitudes of different "peripherality"; along these lines one can go from the very simple ansatz of Eq. (3) to refined -- but not well-defined -- models describing the nature of the singularities which dominate elastic scattering at high energies. We believe that at present the first "optical" approach gives a simpler and more satisfactory description of the process under discussion.

3. ELASTIC SCATTERING AT LARGE MOMENTUM TRANSFERS

Results on elastic scattering at large momentum transfers have recently been obtained by the ACGHT Collaboration[23]. The set-up is sketched in Fig. 5. To distinguish the few elastic events at large momentum transfer from the inelastic background, the momenta of the outgoing particles are determined by measuring the momenta in two magnets placed one above and the other below the ISR vacuum chamber. The trajectory of each proton is defined by three magnetostrictive modules, one of which is placed at the centre of the magnet. The angular range covered by the apparatus is 30-100 mrad, which implies a detected maximum momentum transfer which increases with energy, going from 1.5 GeV^2 to 7 GeV^2 when the ISR momentum varies between 11.8 GeV/c and 26.5 GeV/c.

In Fig. 6 the momentum of one of the detected particle p_1 is plotted versus the momentum of the other particle p_2. A clustering due to elastic events ($p_1 = p_2$) is clearly seen, together with bands due to the events in which one of the protons remains unchanged while the other gets excited.

The elastic events are defined as events in which: i) the closest distance of approach is < 10 mm (the r.m.s. value of this quantity is $\sim$ 1.5 mm); ii) the momenta are equal to the incoming momenta within ±3 GeV/c (the momentum resolution of the magnets is 2%); iii) the two tracks are collinear within ±2.5 mrad. In spite of the wide cuts used there is no problem in identifying elastic events.

A preliminary differential cross-section obtained at (26.6 + 26.6) GeV/c (i.e. at 1500 GeV/c equivalent laboratory momentum) is shown in Fig. 7. The estimated normalization error is at present 20%. In the figure the angular distributions measured at the CERN PS by the CERN-Rome Collaboration[13] and other low-energy results are also plotted. The ACGHT Collaboration has also measured elastic scattering at the three lower ISR energies. Comparing the momentum transfer dependence of the differential cross-section at the four typical ISR energies, the authors conclude that the behaviour of $d\sigma/dt$ above $t \simeq 0.3$ GeV^2 changes very little when the energy is varied in the range available to the ISR. In particular, the position of the minimum moves, if anything, by less than ~ 0.1 GeV^2 going from $\sqrt{s} = 31$ to 53 GeV. Since at present the normalization is uncertain to 20%, this is the accuracy with which one can say that the cross-sections at different energies not only have the same behaviour but also the same absolute value.

Comparing the ISR results with lower energy data, it appears from Fig. 7 that, when the laboratory momentum increases from 30 GeV/c to 1500 GeV/c, the well-known structure present at $t \simeq 1.4$ GeV^2 develops in a clear minimum, a feature which is common to most diffraction phenomena.

A review of the various models proposed to explain the origin of the structure has recently been published by the CERN-Rome Collaboration in connection with scattering data obtained at the CERN PS[13], so that here the discussion will be short and limited to some Regge models and to the optical model of Chou and Yang. In connection with the first class of models, the ISR data disagree with the predictions of Frautschi and Margolis[24], who made use of a multiple scattering formalism to generate corrections to a model in which the Pomeranchuk trajectory has slope 0.8 GeV^{-2}. The same can be said for the model of Greco[25], in which the Pomeron pole and its cuts are described by means of a Veneziano formula.

The optical model calculation by Durand and Lipes[26] is based on the idea of Chou and Yang, and is in good agreement with the ISR data, as recent calculations performed along the same line show[27,28]. The results of one of these calculations[28] are compared in Fig. 8 with the preliminary data of the ACGHT Collaboration.

As is usually the case, a dipole formula with $\mu^2 = 0.71$ GeV^2 has been used as the form factor of hadronic matter. The model predicts a minimum at the correct momentum transfer and the height of the secondary maximum is not very different from the measured one. However, the model predicts a second diffraction minimum at $|t| \simeq 4$ GeV^2, which is not seen experimentally, and the secondary maximum is sensitive to the value of the total cross-section (which in the figure is taken to be $\sigma_t = 40$ mb).

The data shown in Fig. 7 are also in reasonably good agreement with the "hybrid model" of Chiu and Finkelstein[29], in which the asymptotic distribution of Durand and Lipes is thought to be dynamically generated by a fixed Pomeranchuk pole plus cuts. To this contribution the effect of normal Regge singularities is added to generate the energy dependence.

Combining these observations with the conclusion reached in the previous section, one can say that a quite simple optical model à la Chou and Yang semiquantitatively reproduces both the t-dependence of the slope parameters b at small momentum transfers and the high momentum transfer behaviour of the differential cross-sections, as measured at centre-of-mass energies larger than $\sqrt{s} \simeq 25$ GeV. However it must be stressed that the model, in its simple and appealing form, is applicable only at infinite energy, and *ad hoc* hypotheses have to be introduced to justify the way in which the limiting behaviour of the cross-section is reached.

4. PROTON-PROTON SCATTERING IN THE COULOMB REGION

The CERN-Rome Collaboration has performed an experiment on proton-proton scattering in the Coulomb region[30] with two aims: i) to obtain a value for the total proton-proton cross-section σ_t with errors of the order of 2%; ii) to determine the ratio ρ of the real to the imaginary part of the nuclear amplitude (error $\Delta\rho \simeq 0.05$).

In this experiment an unnormalized elastic angular distribution N(t) of the number of events versus t is measured at very small momentum transfers ($0.001 \leq |t| \leq 0.015$ GeV^2). In this range Coulomb scattering is important and, since the Coulomb amplitude is known as a function of t, the scale of the elastic differential cross-section can be fixed. The procedure applied in analysing the data can be logically

subdivided in four steps: i) by using the known Coulomb cross-section, one obtains from the unnormalized angular distribution N(t) the differential cross-section $d\sigma/dt$ (the accuracy of the procedure depends upon the amount of Coulomb scattering which is present in the first measured points, i.e. depends upon the minimum momentum transfer detected). ii) By fitting the form of $d\sigma/dt$ one obtains the value of ρ, which is the ratio of the real to the imaginary part of the nuclear amplitude. iii) By assuming the experimental behaviour e^{-bt} discussed in the previous section, the nuclear contribution to the differential cross-section $(d\sigma/dt)$ is extrapolated to $t = 0$. iv) By applying the optical theorem, from $(d\sigma/dt)_{t=0}$ one gets $\sigma_t(1 + \rho^2)^{\frac{1}{2}}$ and, since ρ is known from step (ii), eventually one obtains the total cross-section σ_t.

In practice, as will be seen in the following, these logical steps are performed as parts of a single fitting procedure. However, they are useful for pointing out two important facts: i) from a measurement in the Coulomb region one can obtain σ_t without any need of a determination of the machine luminosity; ii) the accuracy of the method improves as the minimum momentum transfer detected by the apparatus decreases, since the ratio of the Coulomb to the nuclear contributions increases proportionally to t^2.

For a total cross-section equal to 40 mb the angle at which the Coulomb and the nuclear amplitudes are equal is

$$\theta^\circ_{\text{mrad}} \simeq \frac{42}{p_{\text{GeV}}}, \tag{8}$$

so that $\theta^\circ = 3.4$ and $\theta^\circ = 2.8$ mrad for colliding beams of 11.8 and 15.5 GeV, respectively. To reach scattering angles as small as 2 mrad, four systems of counters are mounted in very thin movable "pots" which are introduced into the vacuum chamber after the proton beams have been stacked (Fig. 9). Two pairs of hodoscopes are thus placed above and below the circulating beams at about 9 m from the point in which the two beams cross. The typical distance in the vertical plane at which the bottom of a pot can be placed from the axis of the machine without disturbing the circulating beam is $\sim$ 15 mm. (Beams of 3-5 A have a typical height of 4 mm FWHM.) The edge of the first hodoscope counter is

thus at 18-20 mm from the axis and the minimum angle is $\sim$ 2 mrad. Given this minimum angle, a sizeable contribution due to the Coulomb amplitude can be detected, according to Eq. (8), when the beam momenta are not too high. Indeed data have been collected at (11.8 + 11.8) GeV/c and at (15.5 + 15.5) GeV/c, which are the two lowest standard ISR momenta.

Each of the four hodoscopes consist of 12 scintillation counters and two trigger counters (Fig. 9). The coincident events between pairs of opposite hodoscopes (AB and CD) are recorded on tape through a small on-line computer. Elastic events are distinguished from inelastic events through a collinearity condition: they are recorded on homologous (or almost homologous) counters of the opposite hodoscopes. The dimensions of the source and of the counters are such that the r.m.s. value of the collinearity angle in the vertical plane is ± 0.25 mrad. Within this collinearity the inelastic event contribution is $\sim$ 1% of the elastic rate and can be easily subtracted. In Fig. 10 two typical angular distributions obtained in runs of a few hours each are shown after some corrections ($\sim$ 3%) have been applied to the data. The main sources of these corrections are the finite length of the sources and the betatron angles within the beams.

To obtain the values of the total cross-section σ_t and of the ratio ρ of the real to the imaginary parts of the forward nuclear amplitude the rate of elastic events N(t) is written as:

$$N(t) = K \left[\left(\frac{2\alpha}{t} \right)^2 G^4(t) - (\rho + \alpha\Phi) \frac{\alpha}{\pi} \sigma_{tot} \frac{G^2(t)}{|t|} e^{\frac{1}{2} bt} + \left(\frac{\sigma_{tot}}{4\pi} \right)^2 (1 + \rho^2) e^{b t} \right], \tag{9}$$

where K is an unessential proportionality constant and $\alpha \simeq 1/137$.

The first term is the well-known Coulomb cross-section when one takes into account also the electromagentic form factor of the interacting protons

$$G(t) = \frac{1}{\left(1 + \frac{t}{\mu^2}\right)^2} \quad \text{with } \mu^2 = 0.71 \text{ GeV}^2 .$$

The second term is the interference between the nuclear amplitude and the Coulomb contribution, which has the phase $\alpha\Phi$. For this phase the expression given by Locher[31] and by West and Yennie[32] is used. Note that $\alpha\Phi$ is always small ($\alpha\Phi \simeq 2.5 \times 10^{-2}$) so that its numerical value does not affect the determination of σ_t.

The third term in Eq. (9) is the nuclear contribution. In writing it the assumption is made that ρ does not depend upon t and that the t-dependence of the imaginary part is exponential. These assumptions are consistent with the results discussed in the previous section and with data obtained at lower energies.

Another assumption is involved in the choice made for the nuclear amplitude: spin effects are negligible. This is justified by the fact that they are already small at 1.5 GeV/c laboratory momentum and are not likely to increase with energy. The validity of this assumption has also been independently confirmed by applying Eq. (9) to scattering data collected at the CERN PS and in Serpukhov, and by checking that the best fitted value of σ_t agrees with the results obtained in transmission experiments.

Since b is a very insensitive parameter and can be taken from the measurements at larger momentum transfer discussed in the previous section, Eq. (9) contains three parameters (K, σ_t, and ρ) which can be determined by fitting the data.

The best fitted values of σ_t and ρ appear in Table 4. In the last column the elastic cross-section σ_{el} is given. It is deduced from the value of the forward elastic cross-section $(d\sigma/dt)_{t=0}$ and from the shape of the angular distribution discussed in the previous section.

Table 4

Total cross-section, real part and elastic cross-section obtained by the CERN-Rome Collaboration[30]

ISR momenta (GeV/c)	Equivalent laboratory momentum (GeV/c)	σ_t (mb)	ρ	σ_{el} (mb)
11.8	290	38.9 ± 0.7	+0.02 ± 0.05	6.7 ± 0.3
15.4	500	40.2 ± 0.8	+0.03 ± 0.06	6.9 ± 0.4

The results on σ_t will be discussed in the next section. In Fig. 11 the values of ρ are plotted, together with data at lower energies[33]. The continuous line represents the prediction of a dispersion relation calculation in which 40 mb is assumed as a common value for the proton-proton and antiproton-proton cross-sections.

Our results do not disagree with this calculation, but would prefer a solution in which the real part crosses zero in the ISR energy range. Taking the average of the two numbers, one indeed gets

$$s \simeq 750 \text{ GeV}^2 , \quad \rho = +0.025 \pm 0.035 , \tag{10}$$

which is about two standard deviations away from the range of values predicted by unsubtracted dispersion relations in which the asymptotic proton-proton and antiproton-proton cross-sections are assumed to converge to common values not very different from 40 mb. This point will be discussed further in Section 7.

In conclusion, this measurement shows that in the ISR energy range the forward nuclear amplitude is essentially imaginary, as expected in diffractive phenomena.

5. TOTAL CROSS-SECTIONS WITH THE VAN DER MEER METHOD*)

Two other approaches are used at the ISR to measure total cross-sections. Both of them apply the method proposed by Van der Meer[34] to obtain the machine luminosity L, which by definition is the proportionality factor between a cross-section $\Delta\sigma$ (integrated over the solid angle of the apparatus) and the corresponding rate R:

$$R = L \cdot \Delta\sigma . \tag{11}$$

The Pisa-Stony Brook Collaboration[35] with the set-up shown in Fig. 12 counts the total number of proton-proton interactions over a large fraction of the whole solid angle. From this measurement the rate R_t, extrapolated to the whole solid angle, is obtained, and the total cross-section is deduced by applying Eq. (11):

---

*) The contents of this and the following section have been updated to February 1973.

$$\sigma_t = \frac{R_t}{L} . \qquad (12)$$

The extrapolation (which is of the order of 5%) is needed to correct for elastic and quasi-elastic events which are lost because the charged particles do not come out of the vacuum chamber.

The second approach has been first applied by the ACGHT Collaboration[36] and can be subdivided in the following four steps:

i) measurement of the elastic rate $R_{el}(\Theta)$ in the solid angle $\Delta\Omega$ at some small scattering angle Θ;

ii) extrapolation of the elastic rate, with the usual exponential behaviour of Eq. (1), to zero angle to get $R_{el}(0)$;

iii) application of Eq. (11) to deduce the elastic cross-section in the forward direction:

$$\left(\frac{d\sigma}{d\Omega}\right)_{0^\circ} = \frac{R_{el(0)}}{L \cdot \Delta\Omega} ; \qquad (13)$$

iv) use of the optical theorem to derive σ_t:

$$\sigma_t = \frac{4\pi\hbar}{p} \sqrt{\left(\frac{d\sigma}{d\Omega}\right)_{0^\circ}} . \qquad (14)$$

This approach has recently been applied by the CERN-Rome Collaboration[37] introducing the hodoscopes shown in Fig. 13 in the "pots" previously described in connection with the Coulomb experiment. The scattering angle is $\Theta \simeq 6$ mrad.

In both approaches the main error comes from the measurement of the machine luminosity, but the second method is less sensitive to errors in L since, from Eqs. (13) and (14),

$$\sigma_t \propto \sqrt{\frac{d\sigma}{d\Omega}} \propto \sqrt{\frac{1}{L}} .$$

In any experiment the time-variation of the luminosity is followed by measuring the rate R_M of a monitor system, which detects beam-beam events without being sensitive to the position and the dimensions of the

crossing region. If $\Delta\sigma_M$ is the cross-section of the events which are within the acceptance of the monitor system, from Eq. (11) it follows that

$$L = \frac{R_M}{\Delta\sigma_M} , \tag{15}$$

and the luminosity to be introduced in Eqs. (12) and (13) can be computed if the "monitor constant" $\Delta\sigma_M$ has been measured, for instance with the Van der Meer method.

The principe of the method[34] consists in displacing the two beams vertically in small and known steps, and in measuring the monitor rate $R_M(\delta)$ as a function of the displacement δ. Given the vertical density distributions $i_1(z - z_1)$ and $i_2(z - z_2)$ of the stored beam currents, one can write:

$$R_M(\delta) = \frac{\Delta\sigma_M}{e^2 c \ \mathrm{tg}\left(\frac{\gamma}{2}\right)} \int_{-\infty}^{+\infty} i_1(z) i_2(z + \delta) \, dz , \tag{16}$$

where $\gamma = 14.8°$ is the crossing angle of the beams in the horizontal plane and $\delta = z_1 - z_2$ is the vertical displacement between the centres z_1 and z_2 of the two beams. From Eq. (16) it is immediately seen that $\Delta\sigma_M$ is proportional to the integral of $R_M(\delta)$, which can be experimentally determined, and inversely proportional to the product $I_1 \cdot I_2$ of the two currents:

$$\Delta\sigma_M = \frac{e^2 c}{I_1 I_2} \mathrm{tg}\left(\frac{\gamma}{2}\right) \int_{-\infty}^{+\infty} R_M(\delta) \, d\delta . \tag{17}$$

The accuracy in the determination of $\Delta\sigma_M$ depends upon the accuracy in the knowledge and in the reproducibility of the scale of the displacements. Typically the steps are $\Delta\delta = 0.50$ mm, and the ISR machine group has measured them at various energies by means of pick-up electrodes, coming to the conclusion that this value has an error $\leq 2\%$, which corresponds to ≤ 0.01 mm.

Checks of this calibration have been performed to an accuracy of $\sim 1\%$ by the Pisa-Stony Brook Collaboration by measuring the vertical displacements of the source with a system of wire chambers.

In the early stages of running of the ISR, the ACGHT Collaboration has published the result of a measurement based on the second of the two approaches discussed above[36]:

$$\sigma_t = (40.2 \pm 2.0) \text{ mb} \quad \text{at} \quad (15.5 + 15.5) \text{ GeV/c} .$$

Data presented at the Batavia Conference by the same group[38] indicated a flat cross-section of (39.3 ± 1) mb up to (26.6 + 26.6) GeV/c.

The recent data of the Pisa-Stony Brook Collaboration[35] (based on the first approach) and of the CERN-Rome Collaboration[37] (who make use of the second approach) are given in Table 5 and are plotted together, with previous data[39], in Fig. 14. As already mentioned, in both experiments the main contribution to the errors comes from an estimated 2% standard deviation on the luminosity, and from an ±2% possible scale error (equal at all energies) on the knowledge of the displacement.

Table 5

Total proton-proton cross-sections

ISR momentum	s GeV^2	Pisa-Stony Brook[36] σ_t (mb)	CERN-Rome[37] σ_t (mb)
(11.8 + 11.8)	550	39.3 ± 0.8	39.1 ± 0.4
(15.4 + 15.4)	935	40.85 ± 0.8	40.5 ± 0.5
(22.6 + 22.6)	2000	42.6 ± 0.85	42.5 ± 0.5
(26.6 + 26.6)	2780	43.0 ± 0.85	43.2 ± 0.6
Scale error		±0.8 mb	±0.6 mb

The agreement between the two sets of results can be considered an indirect check of the validity of the Van der Meer method, since the luminosity enters in different ways in the expressions of the total cross-sections used in the two approaches (in one case σ_t is proportional L^{-1} and in another case to $L^{-\frac{1}{2}}$).

6. RISING TOTAL CROSS-SECTIONS

Many different formulas can be fitted to the increasing behaviour of the total proton-proton cross-section. A particularly simple expression, which represents quite well the data in a large energy interval ($30 \lesssim s \leq 3000$ GeV^2) and is mnemonically easy, is

$$\sigma_t \simeq \left\{38.4 + 0.5 \left[\ln\left(\frac{s}{s_0}\right)\right]^2\right\} \text{ mb} , \tag{18}$$

where s_0 is a well-known number: $s_0 \simeq 137$ GeV^2. For those who like pure numbers, one can also write $\sqrt{s_0} \simeq 4\pi\, m_p$. An expression very similar to Eq. (18) had previously been obtained[40] from an analysis of high-energy cosmic-ray data ($p_L \lesssim 3 \times 10^4$ GeV) concerning the total inelastic cross-section of protons in air.

The rate of increase of Eq. (18) with s is the maximum compatible with the Froissart limit[41], which for $s \to \infty$ has the form:

$$\sigma_t \leq \frac{\pi}{m_\pi^2} \left[\ln\left(\frac{s}{\tilde{s}}\right)\right]^2 , \tag{19}$$

where $\tilde{s}$, the scale of the energies, is unknown. The coefficient of the square of the logarithm in Eq. (19) is ~ 60 mb, i.e. is about 100 times bigger than the fitted value appearing in Eq. (18). This fact poses a problem: In the hypothesis that future data will support representation (18) also at much higher energies, what is the meaning of such a small coefficient? To illustrate this and other connected problems, we present a very simple discussion of the origin and the meaning of the Froissart bound, without any respect for mathematical rigour.

A useful starting point is the usual impact parameter description for the small-angle and high-energy elastic amplitude in the case of scalar particles ($\hbar = 1$):

$$F(s,t) = \frac{1}{\pi} \int d^2a\, e^{i\vec{q}\cdot\vec{a}} f(s,a) , \tag{20}$$

where $q = \sqrt{-t}$ is real in the physical region and $\vec{a}$ is the bivector "impact parameter" in a plane perpendicular to the momenta of the colliding hadrons.

The normalization of the amplitude is such that

$$\frac{d\sigma}{dt} = \pi |F(s,t)|^2 \ , \tag{21}$$

and

$$\sigma_t = 4\pi \ \mathrm{Im}\ F(s,0) \ . \tag{22}$$

To obtain an upper bound for σ_t it is necessary to limit from above the imaginary part of F(s,t), which has a representation similar to that of Eq. (20):

$$\mathrm{Im}\ F(s,t) = \frac{1}{\pi} \int d^2a \ e^{i\vec{q}\cdot\vec{a}} \ \mathrm{Im}\ f(s,a) \ . \tag{23}$$

This bound has to be compatible with the unitarity condition, which states that

$$0 \leq |f(s,a)|^2 \leq \mathrm{Im}\ f(s,a) \leq 1 \tag{24}$$

and with the analyticity properties of F(s,t). These properties follow from microcausality applied to field theory. For our purpose it is only necessary to state the following result[42]: the amplitude sF(s,t) satisfies a dispersion relation also for positive (unphysical) values of t, if t is smaller than a value t_0 which is independent of s. For most scattering processes, t_0 has been demonstrated[43] to be at least

$$t_0 = 4m_\pi^2 \ . \tag{25}$$

For $0 \leq t \leq t_0$ one needs no more than two subtractions in this dispersion relation[44], i.e. sF(s,t) is bounded by s^2 so that

$$\text{for } s \to \infty \quad F(s,t) \simeq Cs^\beta \quad \text{with } \beta \leq 1 \ , \tag{26}$$

where β is in general a function of t.

When $t = t_0$ the two-momentum transfer is imaginary, $q = \pm i\sqrt{t_0}$, and combining Eqs. (23) and (26) one has to satisfy for $s \to \infty$ the condition

$$\frac{1}{\pi}\int da\, d\gamma\; a\; e^{a\sqrt{t_0}\cos\gamma}\; \mathrm{Im}\, f(s,a) \simeq Cs^{\beta}\ , \tag{27}$$

where γ is the angle between $\vec{q}$ and $\vec{a}$. Since the integrand is positive, condition (27) implies, integrating only on a small interval $\Delta\gamma$ around $\gamma = 0$:

$$\frac{\Delta\gamma}{\pi}\int da\; a\; e^{a\sqrt{t_0}}\; \mathrm{Im}\, f(s,a) \leq Cs^{\beta}\ .$$

This condition, which contains the power β computed for $t = t_0$, implies

$$\text{for } a \to \infty \text{ and } s \to \infty \qquad \mathrm{Im}\, f(s,a) \leq \frac{e^{-\sqrt{t_0}\,a}}{(\sqrt{t_0}\,a)^2}\left(\frac{s}{\tilde{s}}\right)^{\beta}\ . \tag{28}$$

Thus, for simplicity forgetting power factors of a, analyticity imposes at the same time an exponential decrease with the impact parameter and a relatively slow rate of increase with the energy ($\beta \leq 1$).

For small values of a and s sufficiently large, the imaginary part of the partial amplitude of Eq. (28) violates the unitarity condition $\mathrm{Im}\, f(s,a) \leq 1$. To obtain a majorant of Eq. (23) which does not violate Eqs. (24) and (28), one can then choose (forgetting power factors)

$$\begin{aligned} &\mathrm{Im}\, f(s,a) = 1 && \text{for } a \leq \bar{a} \\ &\mathrm{Im}\, f(s,a) = e^{-\sqrt{t_0}(a-\bar{a})} && \text{for } a > \bar{a}\ , \end{aligned} \tag{29}$$

where

$$\bar{a} = \frac{\beta\, \ln\,(s/\tilde{s})}{\sqrt{t_0}}\ . \tag{30}$$

Introducing this choice into Eqs. (22) and (23) one finally obtains the upper bound:

$$\sigma_t \leq 8\pi \int_0^{\bar{a}} a\,da + 8\pi \int_{\bar{a}}^{\infty} e^{-\sqrt{t_0}(a-\bar{a})} a\,da$$

$$= \frac{8\pi}{t_0} + \frac{8\pi\beta \ln (s/\tilde{s})}{t_0} + \frac{4\pi\beta^2}{t_0}\left[\ln\left(\frac{s}{\tilde{s}}\right)\right]^2 . \qquad (31)$$

By using the value (25) of t_0 and taking for β its maximum value $\beta = 1$, this result coincides for $s \to \infty$ with the Froissart bound of Eq. (19).

Of course the rough arguments presented above do not prove the Froissart bound, but they show enough resemblance to the steps of the rigorous proof to allow a few relevant comments.

i) The proof relies on the fact that t_0 does not depend upon the energy. This has been shown by Martin to be a consequence of analyticity and unitarity[42]. The value $t_0 = 4m_\pi^2$ is derived from field theory, and of course is a minimum value. (It should be said that for proton-proton scattering a full proof does not yet exist.) Injecting now some phenomenology, if it is known from other sources that the partial amplitude behaves (apart from power factors) as $e^{-\mu a}$, then one can obtain a smaller upper bound for σ_t. For instance, in the Chou and Yang model $\mu^2 = 0.71$ GeV^2 and, if one believes in this model, one has the upper limit

$$t_0 = 0.71 \text{ GeV}^2 , \quad \sigma_t \leq \frac{4\pi\beta^2}{\mu^2}\left[\ln\left(\frac{s}{\tilde{s}}\right)\right]^2 \simeq 7 \cdot \beta^2 \left[\ln\left(\frac{s}{\tilde{s}}\right)\right]^2 \text{ mb} . \qquad (32)$$

ii) In majorating the cross-section the hypothesis has been made that the partial amplitudes which contribute at infinite energy are <u>purely</u> imaginary. The meaning of this hypothesis can be understood by writing for f(s,a) the usual expression, which automatically satisfies the unitarity condition:

$$f(s,a) = \frac{i}{2}\left[1 - e^{2i\delta(s,a)}\right] . \qquad (33)$$

The phase is in general a complex quantity

$$\delta(s,a) = \delta_R(s,a) + i\,\delta_I(s,a) , \qquad (34)$$

and one has

$$\text{Im } f(s,a) = \frac{1 - \cos(2\delta_R)e^{-2\delta_I}}{2} . \tag{35}$$

The choice of Eq. (29) introduced in the maximization procedure means $\delta_R = \pi/2$ and $\delta_I = 0$, which implies that the Froissart bound is obtained in the hypothesis that absorption goes to zero at very high energy. In other words the limit corresponds to a situation in which the inelastic cross-section σ_{in} is zero and the elastic cross-section is equal to the total:

$$\text{with} \quad \text{Im } f(s,a) = 1 \quad \text{for } a \leq \bar{a} \qquad \sigma_{el} = \sigma_t . \tag{36}$$

This seems a quite unphysical situation, since we believe that at very high energy the scattering is essentially diffractive, being due to the absorption of the incoming waves at small impact parameters. Injecting this reasonable diffractive conjecture

$$\delta_R \to 0 , \quad \delta_I \to \infty \quad \text{for } a < \bar{a} , \tag{37}$$

then the unitarity condition gives

$$\text{Im } f(s,a) \leq 1/2 \tag{38}$$

and the Froissart bound is reduced by a factor of 2 [45]. This "reduced" bound will be used in the considerations which follow.

iii) If the total cross-section shows a $\ln^2 s$ behaviour up to very high (infinite) energies, the coefficient in front of the $\ln^2 s$ determines the value of the ratio β^2/t_0. For instance, <u>if the parametrization (18) is applicable as $s \to \infty$</u>, one obtains from the "reduced" bound

$$\frac{\beta^2}{(t_0/4m_\pi^2)} = 0.016 . \tag{39}$$

Thus we have

$$t_0 = 4m_\pi^2 \qquad \beta \simeq 0.13 \ ; \tag{40}$$

$$t_0 = \mu^2 = 0.71 \ \text{GeV}^2 \qquad \beta \simeq 0.38 \ . \tag{41}$$

Since Eq. (40) is a lower limit for β and Eq. (41) is probably an upper one, we conclude that the behaviour of σ_t tells us that the amplitude $sF(s,t)$ (for which dispersion relations are normally written) has a behaviour (for $t = t_0$) which is somewhat between $s^{1.1}$ and $s^{1.4}$. The maximum rate of increase (s^2) would be obtained for $\sqrt{t_0} \simeq 1.4$ GeV.

iv) The first two terms in Eq. (31) give an upper limit for the contribution of the "grey fringe" to the total cross-section, so that for $s \to \infty$ one can write a "reduced" limit

$$\sigma_{\text{fringe}} \leq \frac{4\pi\beta}{t_0} \ln\left(\frac{s}{\tilde{s}}\right) , \tag{42}$$

which is of the order $\ln(s/\tilde{s})$, as expected for a "fringe" of constant width.

v) As remarked under point (ii), in majorating the total cross-section one is lead to choose $\sigma_{el} = \sigma_t$. Very probably this is not the way nature works, and by introducing the diffractive conjecture of Eq. (37) one imposes for $s \to \infty$

$$\sigma_{el} = \frac{\sigma_t}{2} . \tag{43}$$

In the ISR energy range, experimentally[37] we have $\sigma_{el}/\sigma_t \simeq 0.17$, very far from the limit (43). This fact, together with estimates of the cross-section in the fringe based on Eq. (42), show that in the ISR energy range the impact parameter distribution of the amplitude is far from the Froissart bound represented by Eqs. (29) and (30), and also from its "reduced" version, independently of the value chosen for t_0. Thus the mechanism which guarantees a growth of the cross-section not faster than $\ln^2 s$ is not yet effective in this energy range, and we could very well be in a transient situation in which σ_t increases faster than $\ln^2 s$. This implies that the 0.5 mb of Eq. (18) obtained by fitting data in this energy range may not have any deep meaning.

After this detailed discussion of the Froissart bound we briefly review some of the papers in which rising cross-sections have been discussed. As is well known, they constitute a very small sample if compared with the papers in which either constant or decreasing cross-sections have been used or predicted.

Twenty years ago Heisenberg[46] put forward the hypothesis of a proton-proton total cross-section increasing about as $\ln^2 (s/m_\pi^2)$. This was obtained by assuming that the energy density in the interaction decreases as a function of the impact parameter a as $e^{-\mu a}$ and that only impact parameters smaller than a_{max} contribute σ_t. In the model, a_{max} corresponds to a level of the energy density which is approximately constant with s and is fixed by the energy needed to produce two pions. This way of obtaining an increasing cross-section is different from the mechanism discussed in connection with the Froissart bound, and is very similar to what happens in the relativistic rise of the energy losses of charged particles in collisions. In the atomic case a_{max} is determined by the condition that the pulse of electric field applied to the atom by the charged particle must be shorter than the inverse of the characteristic frequencies of the virtual oscillators; a_{max} varies with the energy because of the Lorentz contraction of the electric field.

Regge models in which elastic scattering is dominated by the exchange of a trajectory $\alpha_p(t)$ which has the quantum numbers of the vacuum (Pomeron) give decreasing or constant cross-section according to the choice $\alpha_p(0) < 1$ or $\alpha_p(0) = 1$.

In the simplest single Pomeron exchange model the amplitude is written in the form:

$$F(s,t) = \gamma(t) \exp\left[-i \frac{\pi}{2} \alpha(t)\right] \left(\frac{s}{s_0}\right)^{\alpha_p(t)-1} \qquad (44)$$

where the exponential comes from the signature of the Pomeron trajectory and guarantees that $F(s,t)$ is imaginary when $\alpha_p(0) = 1$. Equation (44) implies that the total cross-section is proportional to $s^{\alpha p(0)-1}$ [see Eq. (22)] and the Froissart bound imposes $\alpha_p(0) \leq 1$.

In general one expects more complicated forms than Eq. (44) to apply. In particular, there is no reason to neglect cut contributions.

Zachariasen has published an excellent review of the subject[47], while Oehme[48] has discussed the implications of rising total cross-sections for the Regge picture of strong interactions. Here we shall present only some of the Regge models which have considered rising cross-sections.

In general one can say that the presence of Regge cuts may produce total cross-sections which increase with energy. The s-dependence is of the form

$$\sigma_t \simeq \sigma_\infty \left[1 - \frac{\xi}{\ln (s/s_0)^\lambda} \right] . \qquad (45)$$

The cut contribution decreases with energy, so that eventually the flat cross-section σ_∞ due to Pomeron exchange dominates, and the usual picture of less and less opaque particles of increasing radius applies.

In the model already discussed, Frautschi and Margolis[24] generated Regge cuts at the form (45) by iterating Pomeron exchange with a Glauber formalism obtaining σ_∞ = 50 mb.

Multiple scattering effects have also been considered by Dean[49] in the framework of a quark model for meson-nuclear scattering. As in all other models, multiple scattering introduces cuts in the angular momentum plane, which disappear with energy and leads to an increase of the total cross-section of several millibarns.

Lendyel and Ter-Martirosyan[50] have applied the Reggeon diagram technique of Gribov[50] to the analysis of the Serpukhov results, predicting a proton-proton cross-section which increases to 68 mb at infinite energy and is slightly larger than the measured values in the ISR energy range.

In their paper[51] on "Rival models for total cross-sections", Barger and Phillips have considered a number of models which can fit the "anomaly" represented at that time by the increasing K^+p cross-section measured at Serpukhov. They consider cut contributions, which give rise to total cross-section of the form (45), and also the effect of adding a dipole to the Pomeron pole. As a third possible model, they add, to the contribution of the Pomeron, a Cheng and Wu term of the type we discuss at the end of this section. In the three models proposed, the predicted increase of σ_t is definitely smaller than the ISR proton-proton results.

Using the Regge model with a fixed Pomeron pole and a "shielding" cut mentioned in Section 2, Barnett[20] has predicted a rising proton-proton cross-section which agrees with the ISR results. The form of the cut is, of course, quite arbitrary, but it has to be mentioned that the model gives also a reasonably good description of the behaviour of the slope of the differential cross-section as a function both of t and s.

A widely used approach to high-energy hadron dynamics is based on the study of the asymptotic behaviour of field theories which can be treated by perturbation methods. (As is well known, analyses of this kind have supported the idea that Regge exchanges dominate hadronic amplitudes.) Local field theories satisfy the main properties which we expect to be valid for the true amplitude: unitarity, analyticity, and crossing symmetry. They can be treated only by partially summing a subset of the whole series of Feyman diagrams, but one can hope that with a careful choice of the summed diagrams the leading contributions are retained and that the high-energy behaviour obtained coincides with the behaviour of the full amplitude. To present in a concise way the main results of these approaches, let us introduce the form (33) of the partial amplitude into Eq. (20). By integrating on the angle γ formed by the bi-vectors $\vec{q}$ and $\vec{a}$, one obtains the well-known expression

$$F(s,t) = i \int da\ a\ J_0(qa) \left[1 - e^{2i\delta(s,a)}\right] . \tag{46}$$

For $a \to \infty$ and $s \to \infty$ the imaginary part of $f(s,a)$ has to satisfy the limitation (28) imposed by the analyticity properties of the full amplitude, so that combining Eqs. (28) and (35) one obtains

$$\frac{1 - \cos(2\delta_R)\ e^{-2\delta_I}}{2} \leq e^{-\sqrt{t_0}a} \left(\frac{s}{\tilde{s}}\right)^{\beta} . \tag{47}$$

In the diffractive limit $\delta_R \to 0$; this implies for $a \to \infty$ and $s \to \infty$:

$$\delta_I(s,a) \leq e^{-\sqrt{t_0}a} \left(\frac{s}{\tilde{s}}\right)^{\beta} , \tag{48}$$

a part power factors in a and logarithmic factors in s.

In conclusion, any theory which satisfies analyticity and unitarity must lead to a phase which satisfies Eq. (47). The most difficult task in the approaches based on the study of the high-energy behaviour of the sum of leading diagrams consists in obtaining the "exponentiated" or "eikonalized" form of Eq. (46) and in deriving the form of the power β appearing in Eq. (48). (Note that the value of t_0 is connected with the mass of the exchanged particle and in general can be considered as a free parameter.)

These difficult problems have been tackled by many authors in various field models. It has been found[52] that in the summation of diagrams where any number of quanta are exchanged between the two external particles one can indeed write the amplitude in the "eikonalized" form of Eq. (46). It turns out that β is equal to the spin of the exchanged quanta minus 1, but that Eq. (48) applies to the real part of the phase $\delta_R(s,a)$ and not to the imaginary part. In other words, these models are completely unrealistic since for $s \to \infty$ they give an elastic amplitude which is non-diffractive, implying $\sigma_{el} = \sigma_t$. This can be understood by noting that, when the coupling constant of the field model goes to zero and the Born term with only one exchange dominates, the eikonal $\delta(s,a)$ is small and the amplitude $F(s,t)$ is proportional to the Fourrier transform of $\delta(s,a)$. Thus the phase $\delta(s,a)$ is essentially the lower order (Born) term of the series. If the model is such that this term is real, then the i in the exponent of Eq. (46) tells us that at very high energy, potential scattering, instead of diffraction scattering, dominates.

Cheng and Wu[53] have considered quantum electrodynamics with massive photons and have summed sets of diagrams which produce a complex phase as $s \to \infty$. In their "impact picture" this is obtained by using as Born term the sum of the "one-tower" diagrams appearing in Fig. 15. These diagrams dominate and are complex, because a ladder is exchanged instead of a single particle, as was done in the field models discussed above. By summing the set of "one-tower" diagrams, Cheng and Wu deduce that the complex phase behaves as $s^d/\ln^2 s$, where d is essentially α^2, the square of the coupling constant appearing in the theory. In electrodynamics, of course, $\alpha = 1/137$, while in any model of strong interactions one expects d to be of the order of 1. Thus in this field model the one-tower diagrams give an absorption which increases as a power of the energy, and

then the arguments discussed above in connection with the Froissart bound apply: the total cross-section increases as $\ln^2 s$ and the elastic cross-section tends to $\sigma_t/2$, as in Eq. (43). It has to be noted that, in order to obtain these results, a very difficult mathematical problem has been solved; it is in fact necessary to prove that the summation of the multitower diagrams (exchange of many towers) does indeed "eikonalize". Conclusions similar to these are obtained by summing similar sets of diagrams in other field theories, as the Φ^3 model, when the coupling constant is large enough[54]. It has been shown by Finkelstein and Zachariasen[55] that also the multiperipheral model, corrected for absorption effects, leads to an amplitude which saturates the Froissart bound at infinite energy.

The previous discussion of the origin of the Froissart bound explains why the same conclusions are common to many different models: the diffractive "reduced" Froissart bound is saturated in any model in which the amplitude is written in the eikonal form of Eq. (46), the phase $\delta(s,a)$ is essentially imaginary when $s \to \infty$ and it is proportional to s^β, with $\beta > 0$. Regge models do not saturate the Froissart bound because, by definition, one requires that at $t = 0$ as $s \to \infty$ the Pomeron exchange amplitude of Eq. (44) dominates. Then $\alpha_p(0) \leq 1$ and also if the Pomeron amplitude is interpreted as a Born term and its Fourrier transform is introduced as eikonal in the representation of Eq. (46) to produce multiple scattering corrections [Frautschi and Margolis[24]], the value of the power $\beta = \alpha_p(0) - 1$ is not larger than zero and one obtains at maximum a constant cross-section reached from below according to Eq. (45).

A parton model which saturates the Froissart bound and connects the increasing cross-section with other phenomena observed in the ISR energy range has been proposed by Kogut, Frye and Susskind[56]. The two colliding hadrons are represented as a uniform population of partons on the rapidity axis covering the region from $-1/2 \ln s$ to $1/2 \ln s$. The number of partons N and their density D (which is assumed to be $D \simeq 2$, as suggested from deep inelastic electron scattering) are simply related:

$$N = D \ln s \simeq 2 \ln s \,. \qquad (49)$$

In the usual descriptions of hadronic processes, the partons interact only within a finite rapidity interval, and this produces a constant total cross-section σ_0 and a multiplicity of the secondaries which increases as ln s. Kogut et al. assume the existence of an additional hard interaction between partons, which has long rapidity range and corresponds to an energy-independent parton-parton cross-section σ_p. Since the number of interacting pairs of partons is $1/2\ N^2$, the contribution of this interaction to the total cross-section is $\sigma_p N^2/2$, and using Eq. (49) the total cross-section can be written in the form

$$\sigma_t \simeq \sigma_0 + 2\sigma_p \ln^2 s \ . \qquad (50)$$

If the representation (18) of the proton-proton data is valid up to very large s, one obtains $\sigma_p \simeq 0.25$ mb, which would naively correspond to a parton radius of $\sim 5 \times 10^{-15}$ cm [57]. The merit of this simple model is in that it relates the increase of the total cross-section with the abundant production of particles of large transverse momenta observed at the ISR, easily understood in terms of a hard interaction.

7. CONCLUSIONS

The main results on elastic scattering and total cross-sections obtained up to February 1973 at the ISR can be summarized as follows.

i) The "local" slope of the elastic differential cross-section changes by $\Delta b \simeq 2$ GeV^{-2} around $|t| = 0.15$ GeV^2.

ii) The forward slope b ($|t| \lesssim 0.15$ GeV^2) increases with energy. A ln s behaviour is not excluded by the existing data, but there are indications that the energy dependence is slower than this. If a ln s behaviour is assumed, b increases by about 10% in the ISR energy range.

iii) The differential cross-section shows a clear minimum at $|t| = 1.4$ GeV^2. Within the present systematic uncertainties on the absolute value of the cross-section (20%), its behaviour does not vary passing from $\sqrt{s} = 31$ to 53 GeV. In the same energy interval, recent data[23] show that the position of the minimum displaces inward by (0.03 ± 0.1) GeV^2.

iv) The real part of the nuclear amplitude in the forward direction is very small ($\rho = 0.025 \pm 0.035$ for $23 \leq \sqrt{s} \leq 31$ GeV).

v) The total proton-proton cross-section increases by (10 ± 2)% in the ISR energy range.

vi) The elastic cross-section, which can be computed from the information summarized in the previous points, increases by (12 ± 4)% in the ISR energy range, if a 10% increase of b is assumed[37]. Indeed one has (apart from corrections of the order of few per cent due to the change of slope around 0.15 GeV^2)

$$\sigma_{el} \propto \frac{\sigma_t^2}{b} , \tag{51}$$

so that a slower increase of b with energy implies a faster increase of the computed value of σ_{el}.

vii) The inelastic cross-section $\sigma_{in} = \sigma_t - \sigma_{el}$ increases in the ISR range by $\sim$ 10% [37], passing from (32.3 ± 0.4) mb to (35.6 ± 0.5) mb.

By stretching some of these data to the limit of their errors [especially point (iii)] one can very naively say that the approximately equal increases of b, σ_t, σ_{el}, and σ_t are compatible with an optical model descriptuon in which the proton-proton interaction radius increases in the ISR energy range by (4 ± 1)%, while the opacity remains constant. However, if the indication of a saturating b and an almost fixed diffraction minimum will be confirmed, then this too simple statement has to be revised.

Looking for a unified picture of the results listed above, the variation of slope of point (i) does not seem to be a very sensitive test. Many different models give it more or less automatically, as discussed in Section 2.

Much more interesting is the energy behaviour of the forward slope, especially in connection with the increasing cross-section. If the total cross-section increases as $(\ln s)^2$, it has been shown[58] that also b must increase at sufficiently high energies at $(\ln s)^2$. As discussed under point (ii), in the ISR energy range this certainly is not the case, but, models which saturate the Froissart bound[53] require this change of behaviour of the slope to happen at energies which at present cannot be reached.

The diffraction minimum observed at $|t| = 1.4$ GeV^2 is very natural in an optical picture of the interactions and is also described by various Regge models. The main point of interest is the variation of the position of the minimum with energy, and its relation to the forward slope. Work on large momentum transfers is in progress, and better data should be available in the near future.

If the total cross-section goes to a constant value of the order of 40 mb, the ratio ρ between the real and the imaginary parts of the nuclear amplitude should always remain negative going to zero from below. However, it is known[59] that, if the cross-section increases as $(\ln s)^2$, ρ must become positive and go to zero from above. Using dispersion relations and making reasonable hypothesis for the high-energy behaviour of the antiproton-proton cross-section, it has been shown[60] that at the maximum ISR momentum ($\sqrt{s} = 63$ GeV corresponding to 2000 GeV/c) ρ varies between +6% and +10% depending on the choice of $\sigma_t \sim \ln s$ and $\sigma_t \sim (\ln s)^2$. Since accurate measurements of the real part are sensitive to the value of σ_t at higher energies, this is the kind of experiment that has to be pursued.

These experiments could give, together with new cosmic-ray data, some hint to answer the fundamental question, Will the proton-proton total cross-section continue to increase, or will it eventually saturate at a large but finite value?

In the first case, a solution in which the Froissart bound is saturated would be very attractive, but very difficult to prove, because also the highest ISR energies have to be considered "intermediate", since the protons are essentially all "fringe". In the hypothesis that nature has chosen this possibility, it will not be easy to discover the mechanism which triggers this behaviour, since many consequences are independent of the mecanism itself but follow from very general principles, as discussed in Section 6. One can also argue that in this case the situation would be simpler, because optics would turn out to be more important than dynamics at very high energies. In the further, not very justified, hypothesis that the representation of Eq. (18) will be valid at much higher energies, the small coefficient that is in front of $(\ln s)^2$ indicates that the range of the absorptive "potential" which produces the saturation

of the Froissart bound is small with respect to the Compton wavelength of a pion. By requiring that the partial amplitudes increase with s at the maximum rate allowed by analyticity and unitarity ($\beta = 1$), one obtains that this range corresponds to exchanges of masses of the order of 1.5 GeV. If all the above hypotheses are satisfied, it is tempting to speculate that this is the mass of the gluons.

If the cross-section saturates at a constant value, a reasonable simplicity will still remain in the Regge description of strong interactions. However, already the observed increase of σ_t poses serious limitations to the properties of the trajectories exchanged in proton-proton and antiproton-proton scattering, and in particular questions the hypothesis of exchange degeneracy[61]. Also in this case the ISR energies are to be considered "intermediate", because cut contributions, which will eventually die, are still important.

In concluding, we remark that it is conceivable that in studying these problems the K^+p system (whose cross-section is already increasing at 20 GeV/c) will turn out to be more useful than the proton-proton system, given the relatively high energy beams available at NAL.

Fruitful discussions with Drs. D. Amati, L. Caneschi, A. Martin, C. Itzykson, M. Jacob, F. Parisi and M. Testa are gratefully acknowledged.

Figure captions

Fig. 1 : Angular distribution of proton-proton elastic scattering at a centre-of-mass energy squared s = 2800 GeV^2 [Aachen-CERN-Harvard-Genova-Torino Collaboration[5)]].

Fig. 2 : Compilation of results on the slope parameter b measured at small momentum transfers[3,5,7)].

Fig. 3 : a) Contributions to elastic scattering in Edelstein model.
b) Contributions to N^* production.

Fig. 4 : Plots of the ratio (ISR data/best fit) using the Chou-Yang model according to White[10)]. The parameters of the dipole form factor are μ^2 = 0.70 GeV^2 and μ^2 = 0.685 GeV^2 at the two energies. The data are taken from Ref. 5.

Fig. 5 : Apparatus used by the Aachen-CERN-Genova-Harvard-Torino Collaboration to detect proton-proton elastic scattering at large momentum transfers.

Fig. 6 : Scattered plot of the momenta of the two charged particles detected in the apparatus of Fig. 5. The clustering due to elastic events is clearly seen.

Fig. 7 : The differential cross-section measured at (26.5 + 26.5) GeV/c by the ACGHT Collaboration is plotted, together with lower momentum data. The numbers accompanying the curves are the laboratory momenta of the incident proton and the dashed curve represents the fourth power of the electromagnetic form factor $G(t) = 1/(1 - t/\mu^2)^2$, with μ^2 = 0.71 GeV^2.

Fig. 8 : The ACGHT data are compared with a calculation due to Moreno and Suaya[28)], based on the optical model of Chou and Yang and Durand and Lipes.

Fig. 9 : Sketch of the "roman pots" and of the counter hodoscopes used by the CERN-Rome Collaboration to detect elastic scattering in the Coulomb region. The pots have stainless steel walls 0.2 mm thick.

Fig. 10 : Angular distributions obtained in two typical runs of a few hours at (11.8 + 11.8) GeV/c and (15.4 + 15.4) GeV/c. The continuous line is the fitted cross-section. The separate contributions of Coulomb and of nuclear scattering are also indicated.

Fig. 11 : Collection of results on the ratio ρ of the real to the imaginary parts of the proton-proton forward scattering amplitude. The two high-energy points are due to the CERN-Rome Collaboration. For the sources of the other data see Ref. 33.

Fig. 12 : Sketch of the apparatus used by the Pisa-Stony Brook Collaboration to measure the total interaction rate due to beam-beam events.

Fig. 13 : The apparatus used by the CERN-Rome Collaboration to measure elastic events around 6 mrad and to obtain the total cross-section using the Van der Meer normalization and the optical theorem.

Fig. 14 : The black points represent recent ISR results on total proton-proton cross-sections obtained by the Pisa-Stony Brook Collaboration (triangles, Ref. 35) and by the CERN-Rome Collaboration (circles, Coulomb normalization, Ref. 30; square, Van der Meer normalization, Ref. 37). The white triangle at 500 GeV/c is the published result of the ACGHT Collaboration[36]. The sources of the other data are collected in Ref. 39.

Fig. 15 : One-tower diagram summed by Cheng and Wu[52] in quantum electrodynamics with massive photons.

REFERENCES

1) M. Holder, E. Radermacher, A. Staude, G. Barbiellini, P. Darriulat, M. Hansroul, S. Orito, P. Palazzi, A. Santroni, P. Strolin, K. Tittel, J. Pilcher, C. Rubbia, G. De Zorzi, M. Macri, G. Sette, C. Grosso-Pilcher, A. Fainberg and G. Maderni, Phys. Letters 35 B, 355 (1971).

2) M. Holder, E. Radermacher, A. Staude, G. Barbiellini, P. Darriulat, P. Palazzi, A. Santroni, P. Strolin, K. Tittel, J. Pilcher, C. Rubbia, M. Bozzo, G. De Zorzi, M. Macri, S. Orito, G. Sette, A. Fainberg, C. Grosso-Pilcher and G. Maderni, Phys. Letters 36 B, 400 (1971).

3) U. Amaldi, R. Biancastelli, C. Bosio, G. Matthiae, J.V. Allaby, W. Bartel, G. Cocconi, A.N. Diddens, R.W. Dobinson, V. Elings, J. Litt, L.S. Rochester and A.M. Wetherell, Phys. Letters 36 B, 504 (1971).

4) R.A. Carrigan, Phys. Rev. Letters 24, 168 (1970).

5) G. Barbiellini, M. Bozzo, P. Darriulat, G. Diambrini Palazzi, G. de Zorzi, A. Fainberg, M.I. Ferrero, M. Holder, A. Mc Farland, G. Maderni, S. Orito, J. Pilcher, C. Rubbia, A. Santroni, G. Sette, A. Staude, P. Strolin and K. Tittel, Phys. Letters 39 B, 663 (1972).

6) U. Amaldi, R. Biancastelli, C. Bosio, G. Matthiae, J.V. Allaby, W. Bartel, M.M. Block, G. Cocconi, A.N. Diddens, R.W. Dobinson, J. Litt and A.M. Wetherell, Contribution to the 16th Int. Conf. on High-Energy Physics, Chicago, 1972.

7) G.G. Beznogikh, A. Buyak, K.I. Iovchev, L.F. Kirillova, P.K. Markov, B.A. Morozov, V.A. Nikitin, P.V. Nomokonov, M.G. Shafranova, V.A. Sviridov, Truong Bien, V.I. Zayacki, N.K. Zhidkov, L.S. Zolin, S.B. Nurushev and V.L. Solovianov, Phys. Letters 30 B, 274 (1969).
Kh. M. Chernev, I.M. Geshkov, N.L. Ikov, P.K. Markov and V.I. Zaiachki, Phys. Letters 36 B, 266 (1971).

8) R.M. Edelstein, 4th Int. Conf. on High-Energy Collisions, Oxford, 1972.

9) B. Carreras and J.N.J. White, Nuclear Phys. B42, 95 (1972).

10) J.N. White, Nuclear Phys. B51, 23 (1973).

11) P. Heckman and R. Henzi, Phys. Letters 41 B, 189 (1972).

12) S. Barshay, Nuovo Cimento Letters 3, 369 (1972).

13) J.V. Allaby, A.N. Diddens, R.W. Dobinson, A. Klovning, J. Litt, L.S. Rochester, K. Schlüpmann, A.M. Wetherell, U. Amaldi, R. Biancastelli, C. Bosio and G. Matthiae, Nuclear Phys. B52, 316 (1973).

14) T.T. Chou and C.N. Yang, Phys. Rev. 170, 1591 (1968), Phys. Rev. Letters 20, 1213 (1968), and Phys. Rev. 175, 1832 (1968).

15) S.Y. Lo and G.D. Thomson, Nuovo Cimento 3, 223 (1972).

16) L. Van Hove, Rev. Mod. Phys. 36, 655 (1964).

17) D.M. Austin and W. Rarita, Phys. Rev. D 4, 3507 (1971).

18) V. Barger, K. Geer and R.J.M. Phillips, Phys. Letters 36 B, 343 (1971).

19) See, for instance: N.G. Antoniou and R. Baier, Phys. Letters 37 B, 501 (1971).
T. Uematsu, Nuovo Cimento Letters 3, 137 (1972).
H. Caprasse, Nuovo Cimento Letters 3, 427 (1972).
J.S. Ball and F. Zachariasen, Phys. Letters 41 B, 525 (1972).
H.W. Meldner and E. Moeller, Phys. Rev. D 6, 390 (1972).

20) R.M. Barnett, Nuclear Phys. B37, 381 (1972).

21) V. Barger, R.J.N. Phillips and K. Geer, Nuclear Phys. B47, 29 (1972).

22) G.L. Kane, Phys. Letters 40 B, 363 (1972).

23) A. Böhm, M. Bozzo, R. Ellis, H. Foeth, M.I. Ferrero, G. Maderni, B. Naroska, C. Rubbia, G. Sette, A. Staude, P. Strolin, G. de Zorzi, to be published.

24) S. Frautschi and G. Margolis, Nuovo Cimento 56 A, 1155 (1968).

25) M. Greco, Phys. Letters 31 B, 216 (1970).

26) L. Durand and R. Lipes, Phys. Rev. Letters 20, 637 (1968).

27) M. Elitzur and R.G. Lipes, An optical model for diffractive resonance production, preprint.

28) H. Moreno and R. Suaya, SLAC-PUB-1161 (TH) December 1972.

29) C.B. Chiu and J. Finkelstein, Nuovo Cimento 57 A, 649 (1968) and 59 A, 92 (1969).

30) U. Amaldi, R. Biancastelli, C. Bosio, G. Matthiae, J.V. Allaby, W. Bartel, M.M. Block, G. Cocconi, A.N. Diddens, R.W. Dobinson, J. Litt and A.M. Wetherell, Phys. Letters B43, 231 (1973).

31) M.P. Locher, Nuclear Phys. B2, 525 (1967).

32) G.B. West and D.R. Yennie, Phys. Rev. 172, 1413 (1968).

33) J.D. Dowell, R.J. Homer, Q.H. Khan, W.K. McFarlane, J.S.C. McKee and A.W. O'Dell, Phys. Letters 12, 252 (1964).
G. Bellettini, G. Cocconi, A.N. Diddens, E. Lillethun, J. Pahl, J.P. Scanlon, J. Walters, A.M. Wetherell and P. Zanella, Phys. Letters 14, 164 (1965).
A.E. Taylor, A. Ashmore, W.S. Chapman, D.F. Falla, W.H. Range, D.B. Scott, A. Astbury, F. Capocci and T.G. Waler, Phys. Letters 14, 54 (1965).
L.F. Kirillova, V.A. Nikitin, V.A. Sviridov, L.N. Strunov, M.G. Shafranova, Z. Korbel, L. Rob, A. Zlateva, P.K. Markov, T. Todorov, L. Khristov, Kh. Chernev, N. Dalkhazhav and D. Tuvdendorzh, Zh. Eksper. Teor. Fiz. 50, 76 (1966) [English translation: Soviet Phys. JETP 23, 52 (1966)]. A compilation of the numerical values from this work is given by O.B. Dumbrais, Yadernaya Fiz. 13, 1096 (1971) [English translation: Soviet J. Nuclear Phys. 13, 626 (1971)].
A.R. Clyde, Univ. Calif. Radiation Laboratory Report UCRL 16275 (1966), unpublished.
K.J. Foley, R.S. Jones, S.J. Lindenbaum, W.A. Love, S. Ozaki, E.D. Platner, C.A. Quarles and E.H. Willen, Phys. Rev. Letters 19, 857 (1967).
L.M.C. Dutton, R.J.W. Howells, J.D. Jafar and H.B. Van der Raay, Phys. Letters 25 B, 245 (1967).
L.M.C. Dutton and H.B. Van der Raay, Phys. Letters 26 B, 679 (1968).
G.C. Beznogikh, A. Bujak, L.F. Kirillova, B.A. Morozov, V.A. Nikitin, P.V. Nomokonov, A. Sandacz, M.G. Shafranova, V.A. Sviridov, Truong Bien, V.I. Zayachki, N.K. Zhidkov and L.S. Zolin, Phys. Letters 39 B, 411 (1972) and Dubna preprint E1-6613 (1972), to be published in Nuclear Phys.

34) Van der Meer, CERN Internal Report ISR-PO/68-31 (1968) (unpublished).

35) S.R. Amendolia, G. Bellettini, P.L. Braccini, C. Bradaschia, R. Castaldi, V. Cavasinni, C. Cerri, T. Del Prete, L. Foa, P. Giromini, P. Laurelli, A. Menzione, L. Ristori, G. Sanguinetti, M. Valdata, G. Finocchiaro, P. Grannis, D. Green, R. Mustard and R. Thun, Phys. Letters (in print).

36) M. Holder, E. Radermacher, A. Staude, G. Barbiellini, P. Darriulat, M. Hansroul, S. Orito, P. Palazzi, A. Santroni, P. Strolin, K. Tittel, J. Pilcher, C. Rubbia, G. De Zorzi, M. Macri, G. Sette, C. Grosso-Pilcher, A. Fainberg and G. Maderni, Phys. Letters 35 B, 361 (1971).

37) U. Amaldi, R. Biancastelli, C. Bosio, G. Matthiae, J.V. Allaby, W. Bartel, G. Cocconi, A.N. Diddens, R.W. Dobinson and A.M. Wetherell, Phys. Letters (in print).

38) Aachen-CERN-Genova-Harvard-Torino data presented by C. Rubbia at the 16th Int. Conf. on High-Energy Physics, Chicago, Sept. 1972. The results presented have been increased by 2% due to a 4% error of the scale of the Van der Meer method which has been discovered later.

39) S.P. Denisov, S.V. Donskov, Yu.P. Gorin, A.I. Petrukhin, Yu.D. Prokoshkin, D.A. Stoyanova, J.V. Allaby and G. Giacomelli, Phys. Letters 36 B, 415 (1971).
J.W. Chapman, N. Green, B.P. Roe, A.A. Seidl, D. Sinclair, J.C. Van der Velde, C.M. Bromberg, D. Cohen, T. Ferbel, P. Slattery, S. Stone and B. Werner, Phys. Rev. Letters 29, 1686 (1972).
G. Charlton, Y. Cho, M. Derrick, R. Engelmann, T. Fields, L. Hyman, K. Jaeger, U. Mehtani, B. Musgrave, Y. Oren, D. Rhines, P. Schreiner, H. Yuta, L. Voyvodic, R. Walker, J. Whitmore, H.B. Crawley, Z. Ming Ma and R.G. Glasser, Phys. Rev. Letters 29, 515 (1972).
F.T. Dao, D. Gordon, J. Lach, E. Malamud, T. Meyer, R. Poster and W. Slater, Phys. Rev. Letters 29, 1627 (1972).

40) G.B. Yodh, Yash Pal and J.S. Trefil, Phys. Rev. Letters 28, 1005 (1972).

41) M. Froissart, Phys. Rev. 123, 1053 (1961).

42) A. Martin, Nuovo Cimento 42, 930 (1966).

43) G. Sommer, Nuovo Cimento 48 A, 92 (1967).
J.D. Bessis and V. Glaser, Nuovo Cimento 58, 568 (1967).

44) L. Lukaszuk and A. Martin, Nuovo Cimento 52 A, 122 (1967), see the Appendix.

45) S.M. Roy, Phys. Reports 5C, 125 (1972).

46) W. Heisenberg, in Kosmische Strahlung (Springer Verlag, 1953), p. 148.

47) F. Zachariasen, Phys. Reports 2, 1 (1971).

48) R. Oehme, Springer Tracts in Mod. Phys. 61, 109 (1972).

49) N.W. Dean, Phys. Rev. 182, 1695 (1969).

50) A.I. Lendyel and K.A. Ter-Martirosyan, JETP Letters 11, 45 (1970).
V.N. Gribov, Soviet. Phys. JETP 26, 414 (1968).

51) V. Barger and R.J.N. Phillips, Nuclear Phys. B40, 205 (1972).

52) For a review see H.D.J. Abarbanel, Cargèse Lectures in Physics, D. Bessis editor (Gordon and Breach, New York-London-Paris, 1971), Vol. 5, p. 519.
S.J. Chang and S.K. Ma, Phys. Rev. Letters 22, 1334 (1969).
H. Abarbanel and C. Itzykson, Phys. Rev. Letters 23, 53 (1969).
M. Levy and J. Sucher, Phys. Rev. 186, 1656 (1969).

53) Cheng and T.T. Wu, Phys. Rev. Letters 24, 1456 (1970); Phys. Letters 34 B, 647 (1971) and Phys. Letters 36 B, 357 (1971). For a recent fit to total cross-sections which has the asymptotic properties of this model see; H. Cheng, J.K. Walker and T.T. Wu "Impact picture of pp, $\bar{p}p$, $\pi^{\pm}p$ and $K^{\pm}p$ elastic scattering from 20 to 5000 GeV", preprint

54) S.J. Chang and T.M. Yan, Phys. Rev. Letters 25, 1586 (1970).

55) J. Finkelstein and F. Zachariasen, Phys. Letters 34 B, 631 (1971).

56) J. Kogut, G. Frye and L. Susskind, Phys. Letters 40 B, 469 (1972).

57) A. Casher, S. Nussinov and L. Susskind, "New effects in the ISR region", preprint TAVP 73-346.

58) A. Martin, Phys. Rev. 129, 1432 (1963).
E. Leader, Phys. Letters 5, 75 (1963).

59) N.N. Khuri and T. Kinoshita, Phys. Rev. 137 B, 720 (1965).

60) C. Bourrely and J. Fischer, CERN-TH 1652 (1973).

61) I thank M. Jacob for this remark.

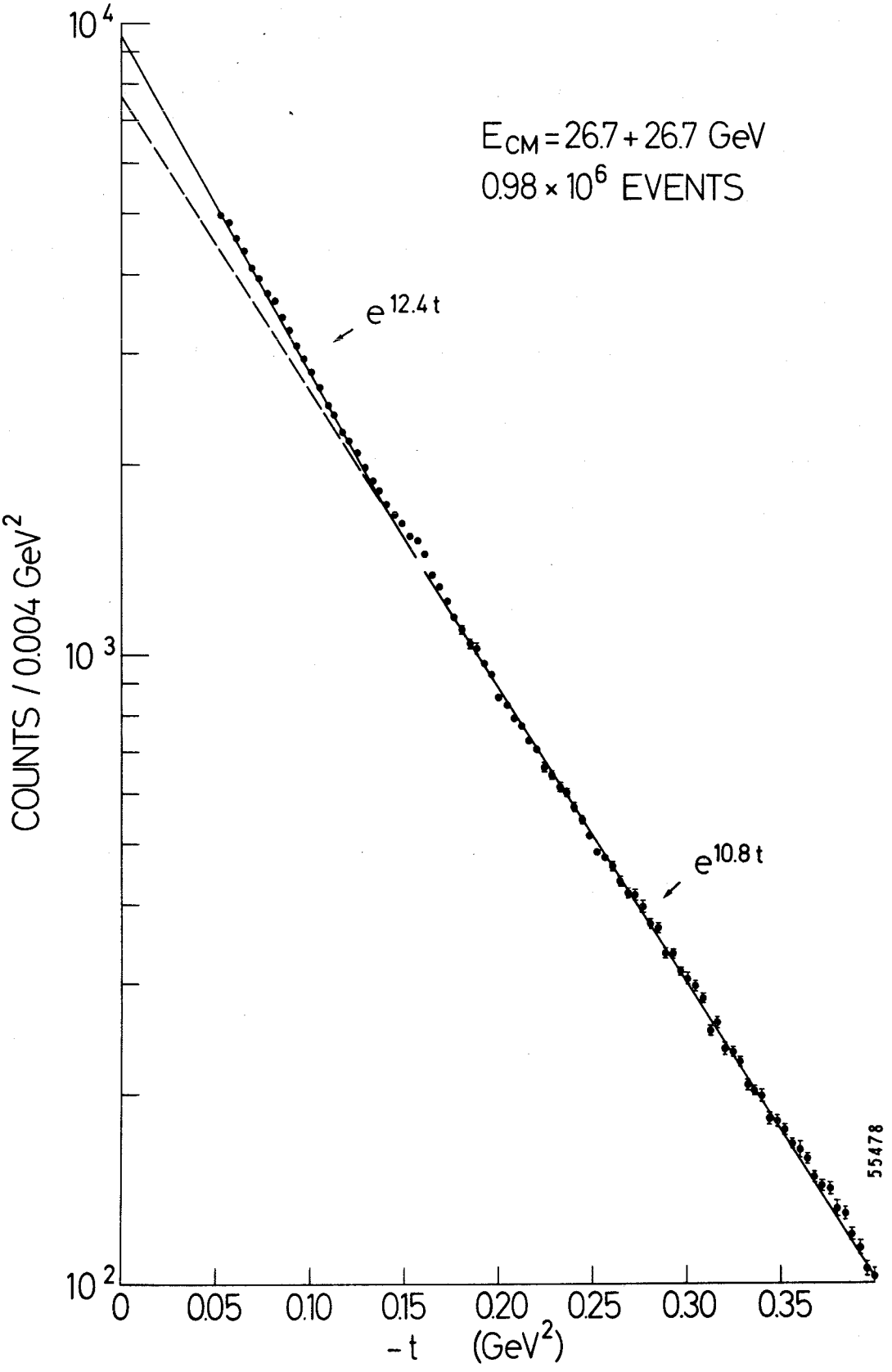
$E_{CM} = 26.7 + 26.7$ GeV
0.98×10^6 EVENTS
$e^{12.4t}$
$e^{10.8t}$
COUNTS / 0.004 GeV^2
10^4
10^3
10^2
0
0.05
0.10
0.15
0.20
0.25
0.30
0.35
$-t$ (GeV^2)
55478

Fig. 1

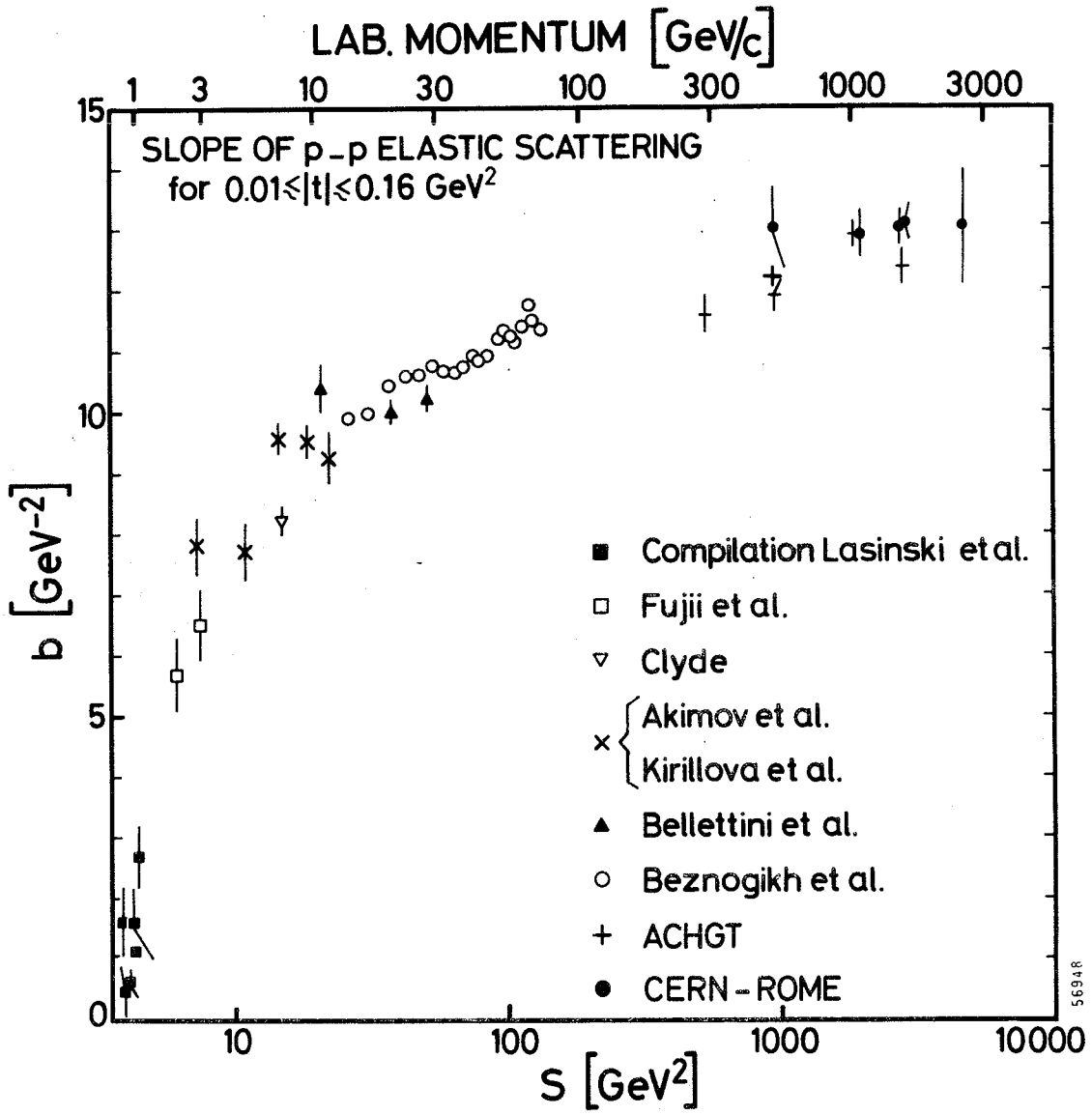
LAB. MOMENTUM [GeV/c]
1
3
10
30
100
300
1000
3000
SLOPE OF p-p ELASTIC SCATTERING
for 0.01≤|t|≤0.16 GeV²
b [GeV⁻²]
15
10
5
0
Compilation Lasinski et al.
Fujii et al.
Clyde
Akimov et al.
Kirillova et al.
Bellettini et al.
Beznogikh et al.
ACHGT
CERN - ROME
10
100
1000
10000
S [GeV²]
5694R

Fig. 2

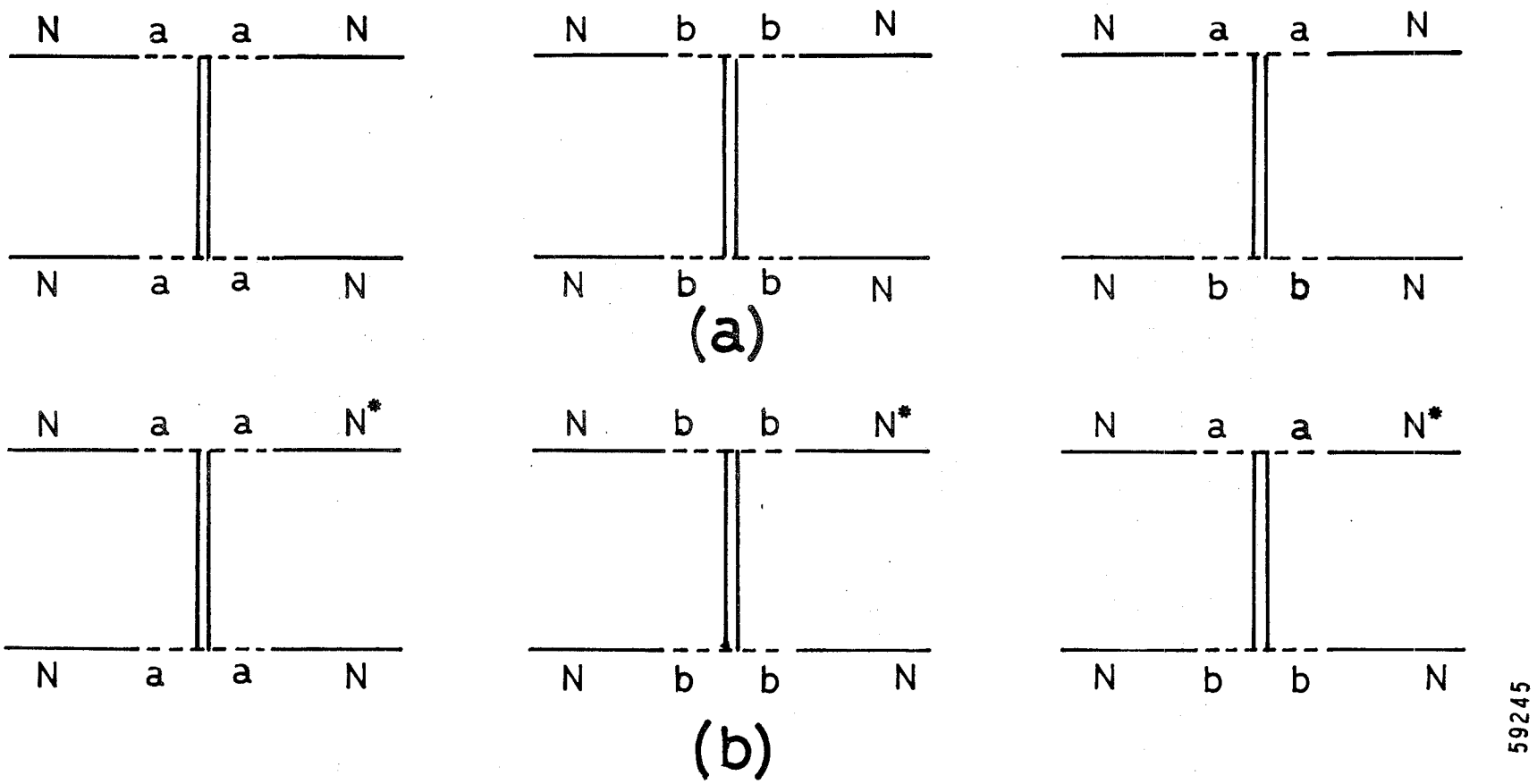
N a a N
N a a N
N b b N
N b b N
N a a N
N b b N
(a)
N a a N*
N a a N
N b b N*
N b b N
N a a N*
N b b N
(b)
59245

Fig. 3

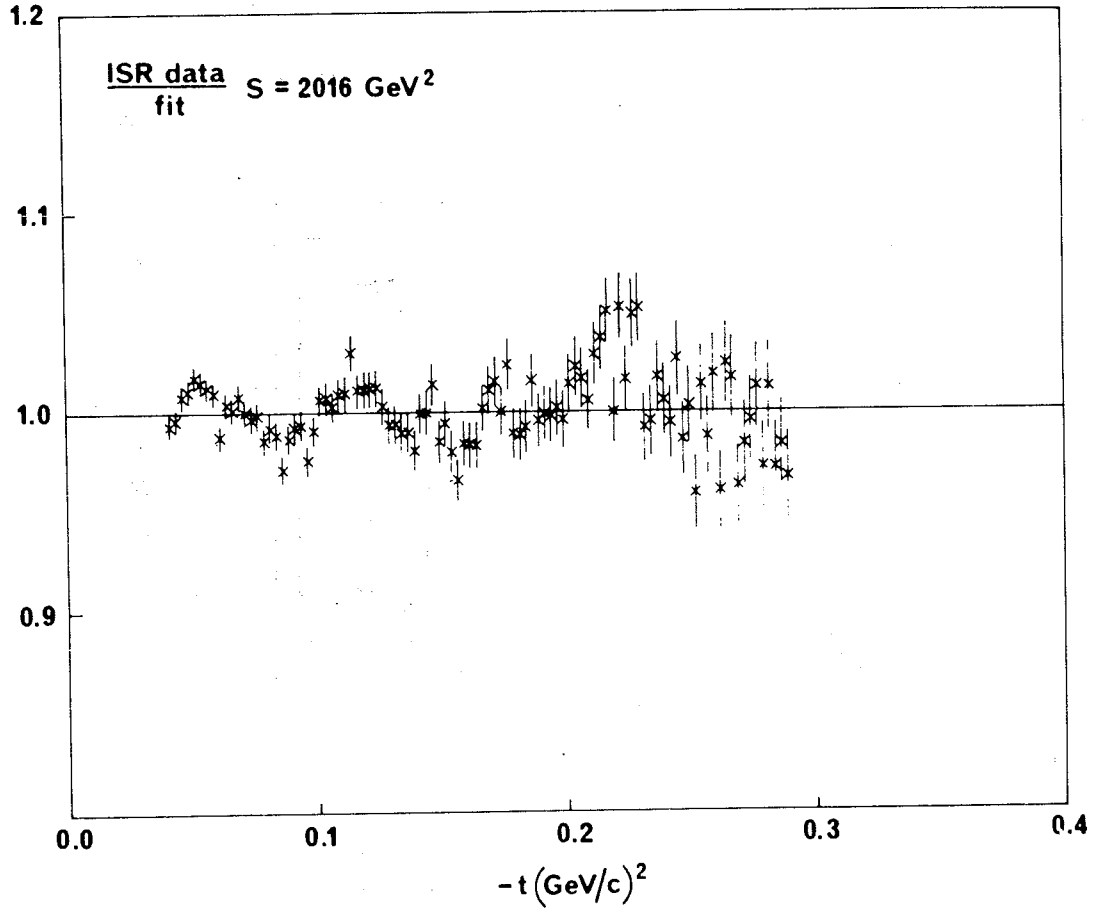
1.2
ISR data / fit
S = 2016 GeV²
1.1
1.0
0.9
0.0
0.1
0.2
0.3
0.4
-t (GeV/c)²

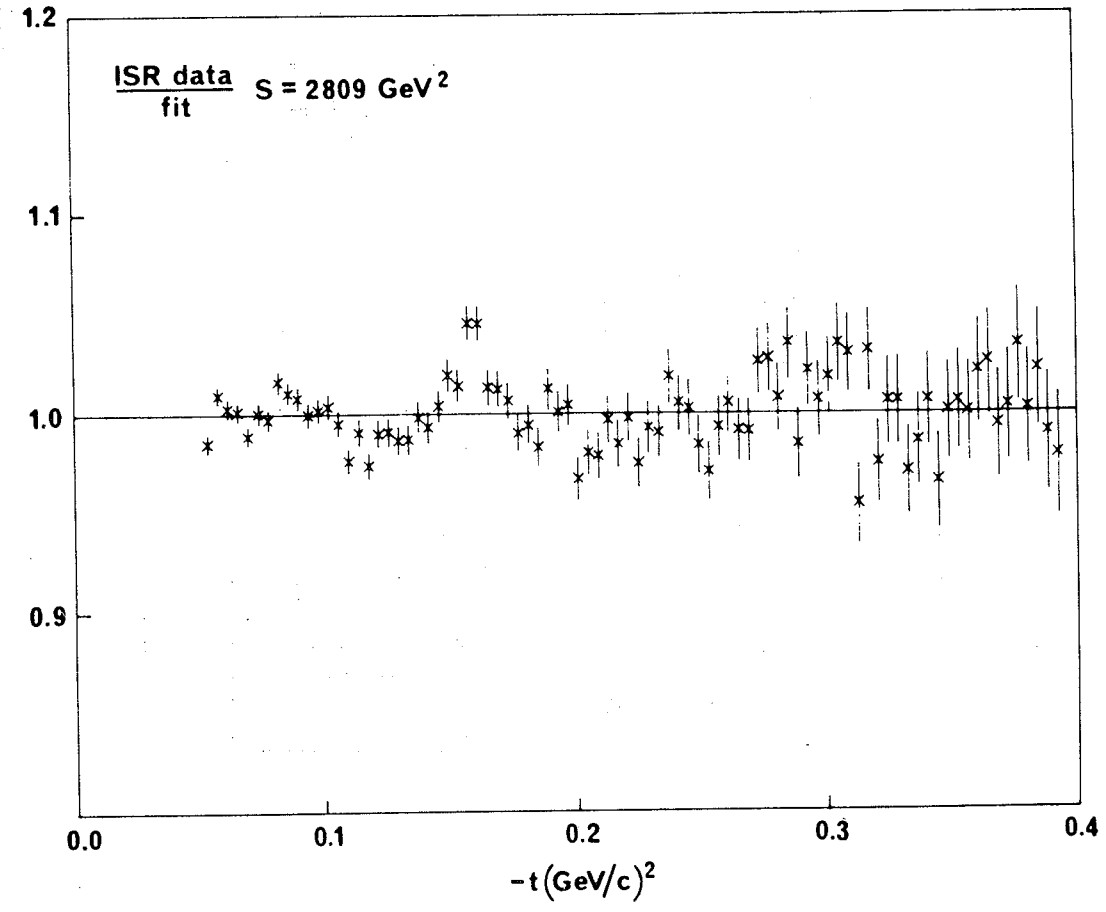
1.2
ISR data / fit
S = 2809 GeV²
1.1
1.0
0.9
0.0
0.1
0.2
0.3
0.4
-t (GeV/c)²

58793

Fig. 4

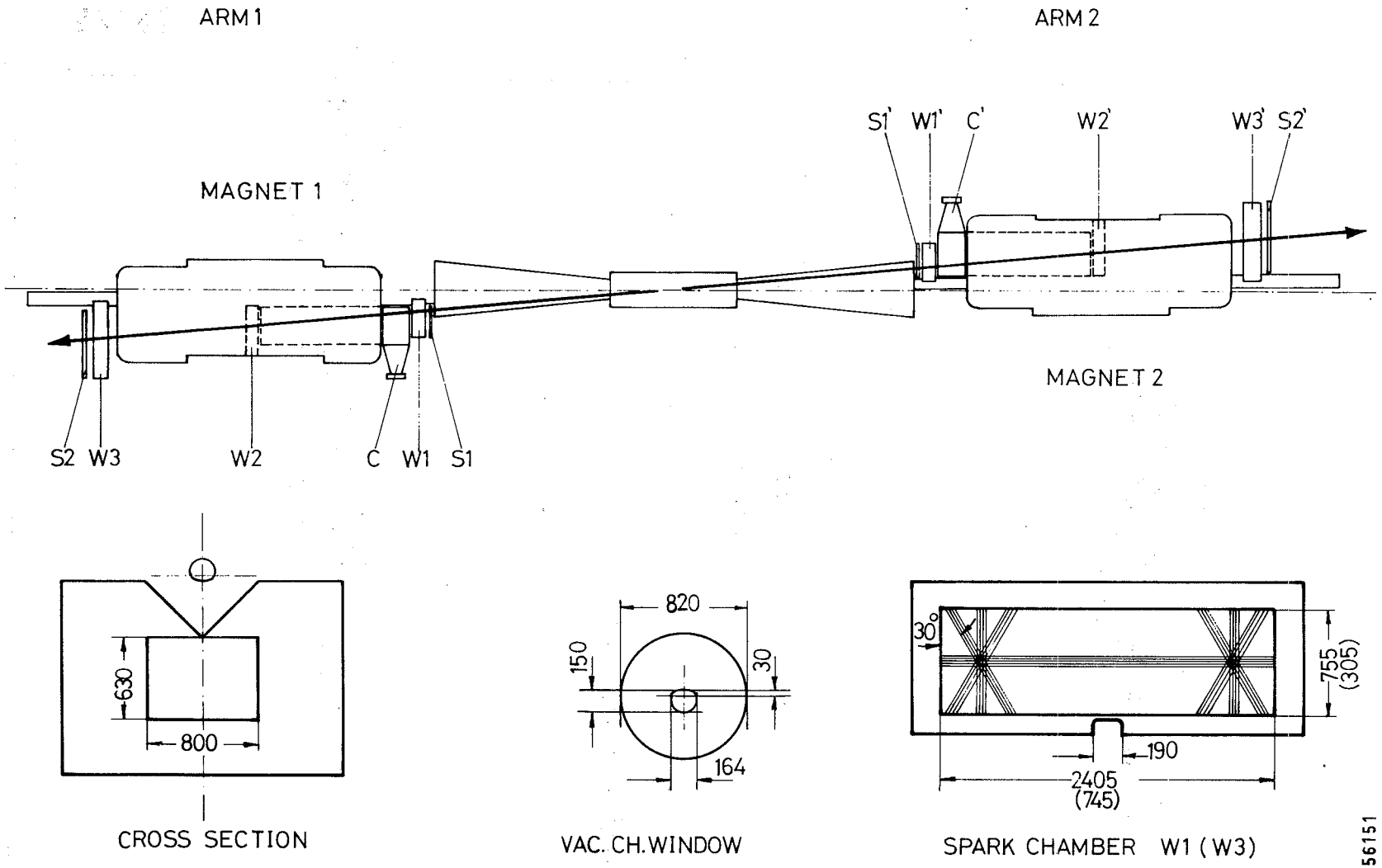
ARM 1
ARM 2
S1' W1' C'
W2'
W3' S2'
MAGNET 1
MAGNET 2
S2 W3
W2
C W1 S1
630
800
CROSS SECTION
820
150
30
164
VAC. CH. WINDOW
30°
755
(305)
190
2405
(745)
SPARK CHAMBER W1 (W3)
56151

Fig. 5

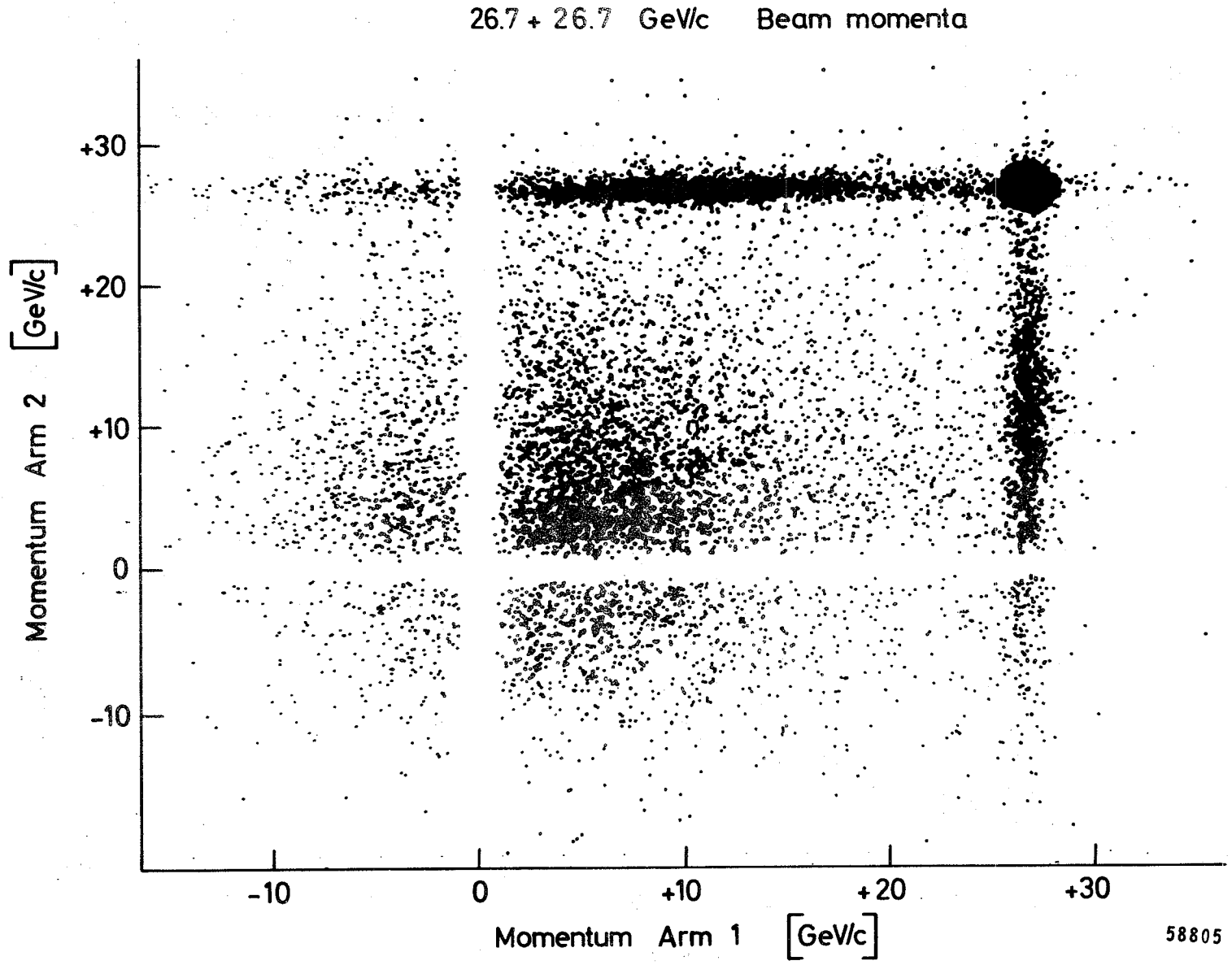
26.7 + 26.7 GeV/c Beam momenta
+30
+20
+10
0
-10
Momentum Arm 2 [GeV/c]
-10
0
+10
+20
+30
Momentum Arm 1 [GeV/c]
58805

Fig. 6

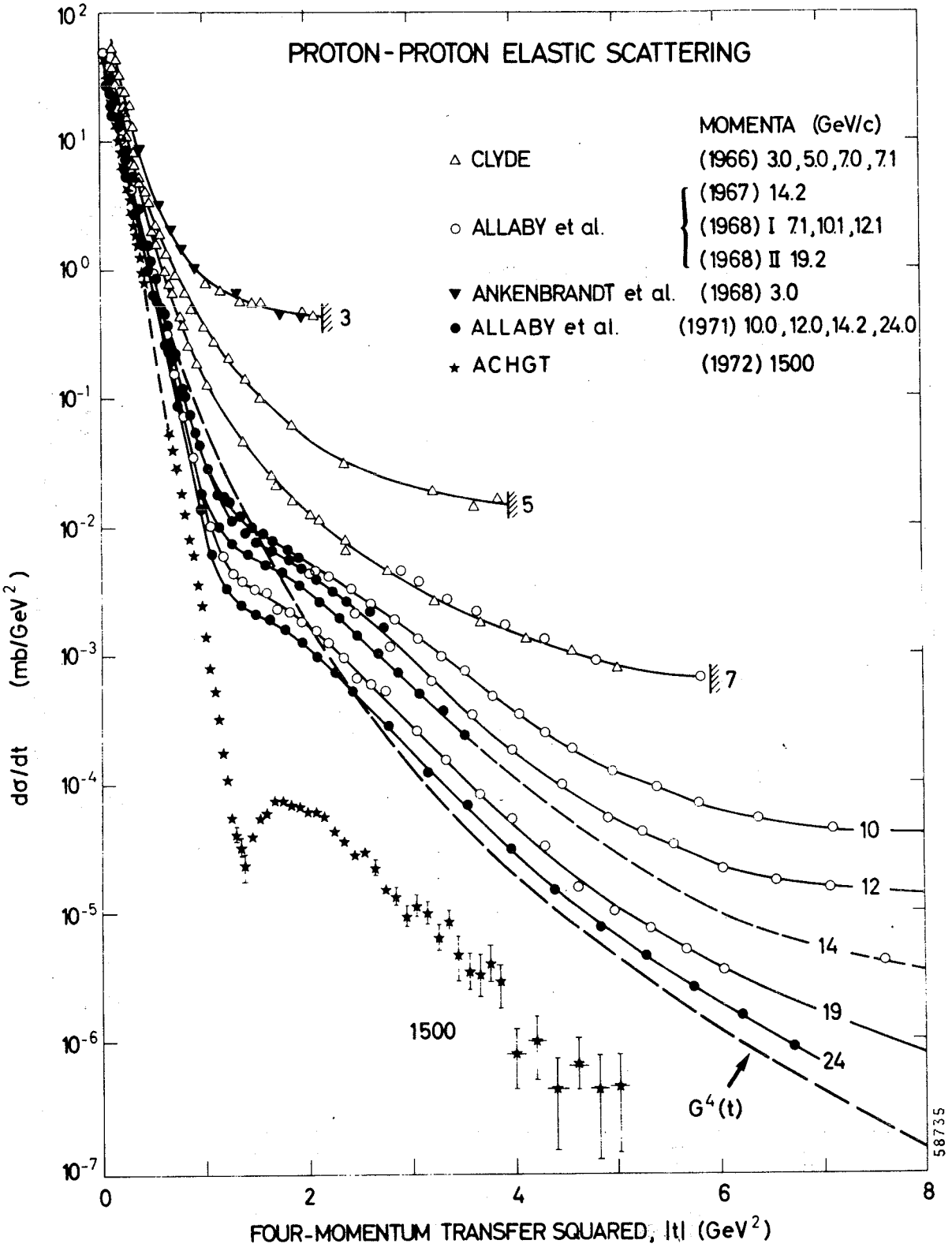
PROTON-PROTON ELASTIC SCATTERING
MOMENTA (GeV/c)
△ CLYDE (1966) 3.0, 5.0, 7.0, 7.1
○ ALLABY et al. (1967) 14.2
(1968) I 7.1, 10.1, 12.1
(1968) II 19.2
▼ ANKENBRANDT et al. (1968) 3.0
● ALLABY et al. (1971) 10.0, 12.0, 14.2, 24.0
★ ACHGT (1972) 1500
3
5
7
10
12
14
19
24
1500
$G^4(t)$
58735
$d\sigma/dt$ (mb/GeV^2)
FOUR-MOMENTUM TRANSFER SQUARED, |t| (GeV^2)
10^2
10^1
10^0
10^{-1}
10^{-2}
10^{-3}
10^{-4}
10^{-5}
10^{-6}
10^{-7}
0
2
4
6
8

Fig. 7

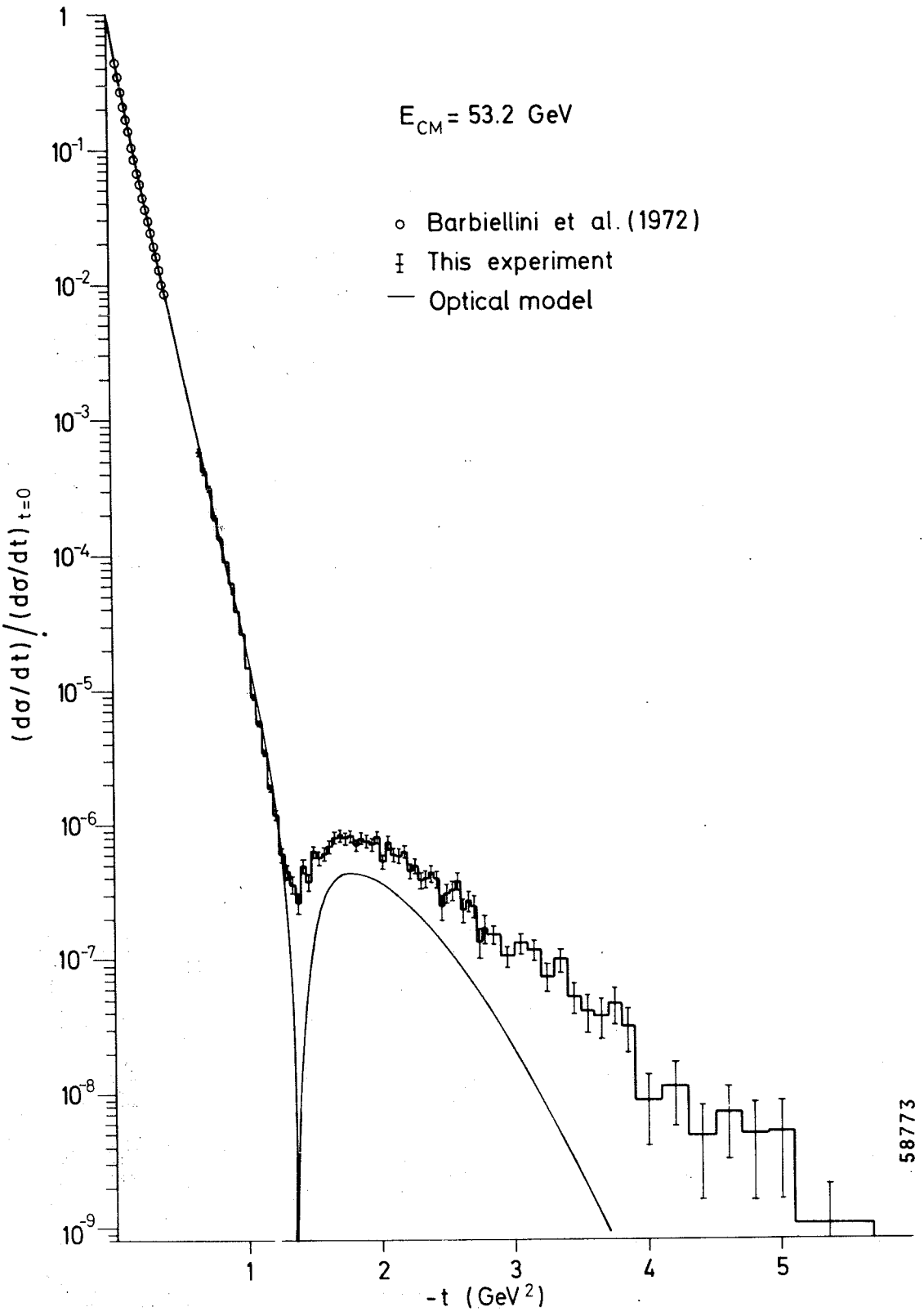
E_{CM} = 53.2 GeV
o Barbiellini et al. (1972)
I This experiment
— Optical model
$(d\sigma/dt)/(d\sigma/dt)_{t=0}$
1
10^{-1}
10^{-2}
10^{-3}
10^{-4}
10^{-5}
10^{-6}
10^{-7}
10^{-8}
10^{-9}
1
2
3
4
5
$-t$ (GeV^2)
58773

Fig. 8

SMALL ANGLE ELASTIC SCATTERING
CERN-ROME

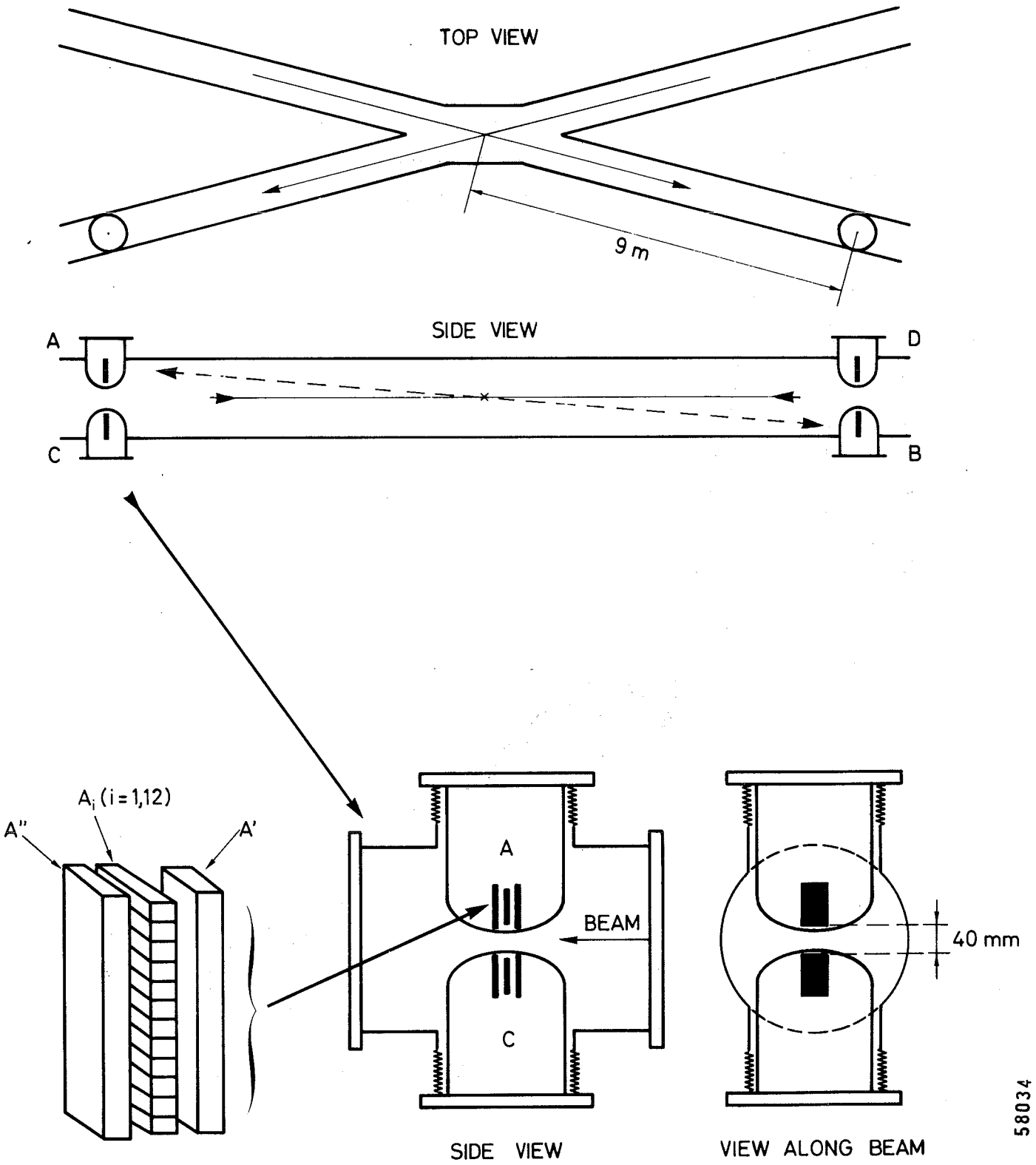

Fig. 9

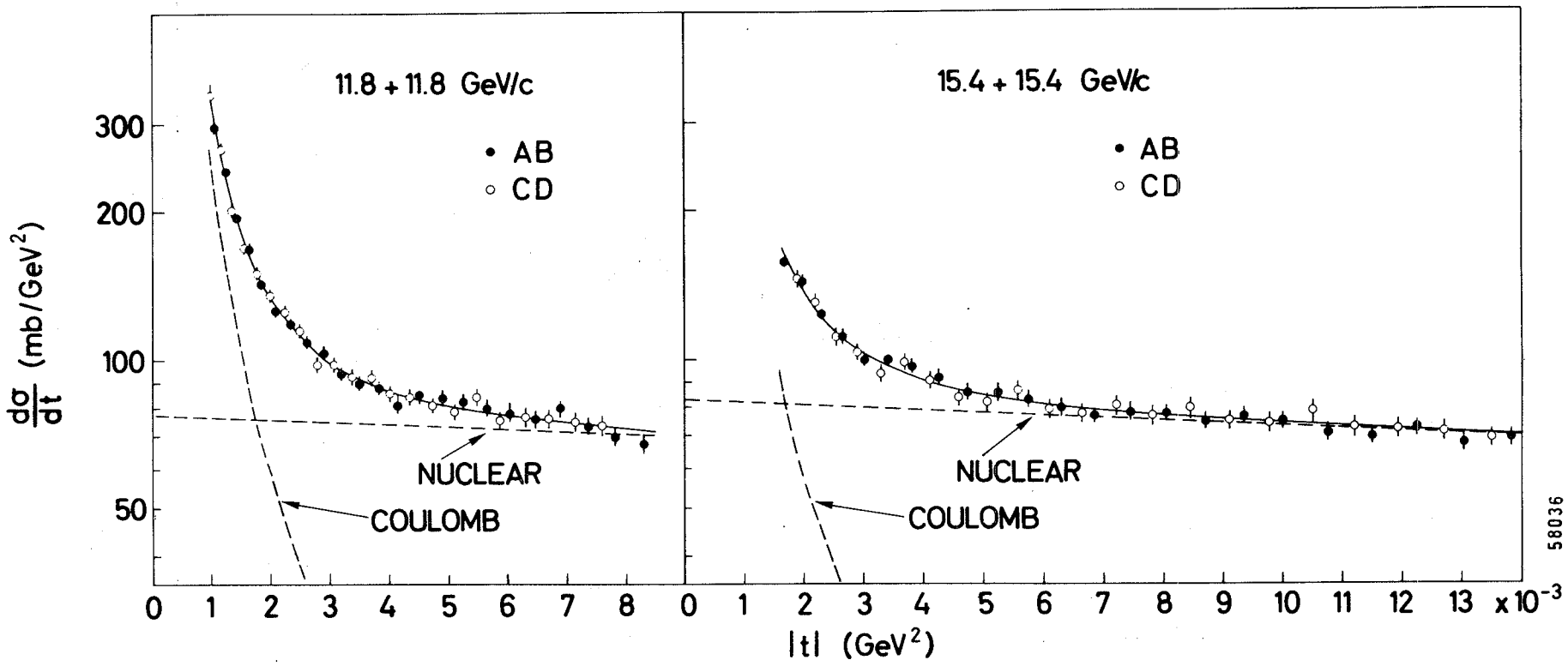
11.8 + 11.8 GeV/c
15.4 + 15.4 GeV/c
• AB
○ CD
NUCLEAR
COULOMB
dσ/dt (mb/GeV²)
|t| (GeV²)
x10⁻³
58036

Fig. 10

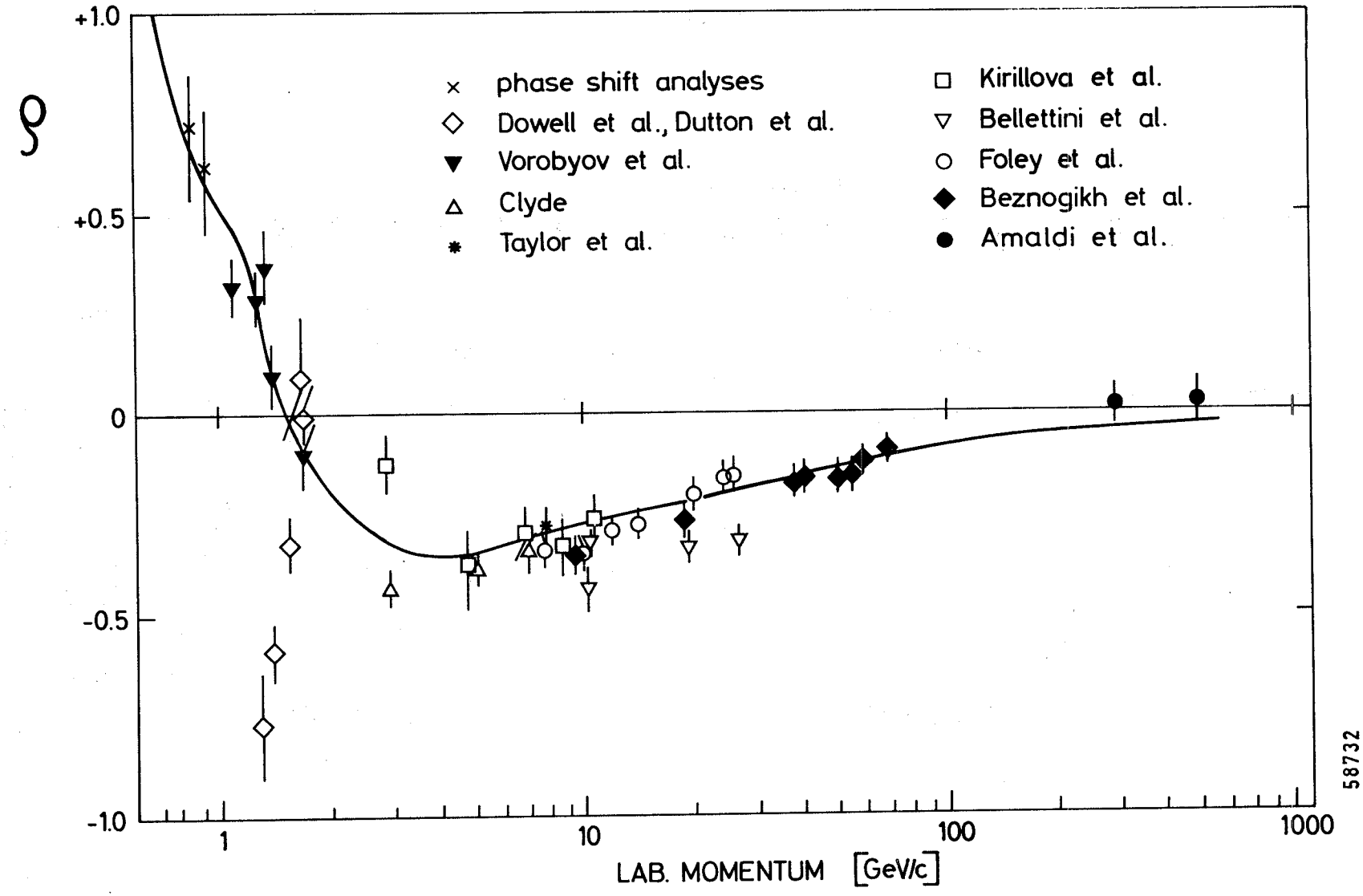
ρ
+1.0
+0.5
0
-0.5
-1.0
1
10
100
1000
LAB. MOMENTUM [GeV/c]
× phase shift analyses
◇ Dowell et al., Dutton et al.
▼ Vorobyov et al.
△ Clyde
* Taylor et al.
□ Kirillova et al.
▽ Bellettini et al.
○ Foley et al.
◆ Beznogikh et al.
● Amaldi et al.
58732

Fig. 11

PISA STONY BROOK

LAY OUT OF THE TOTAL CROSS SECTION EXPERIMENT

(TOP VIEW)

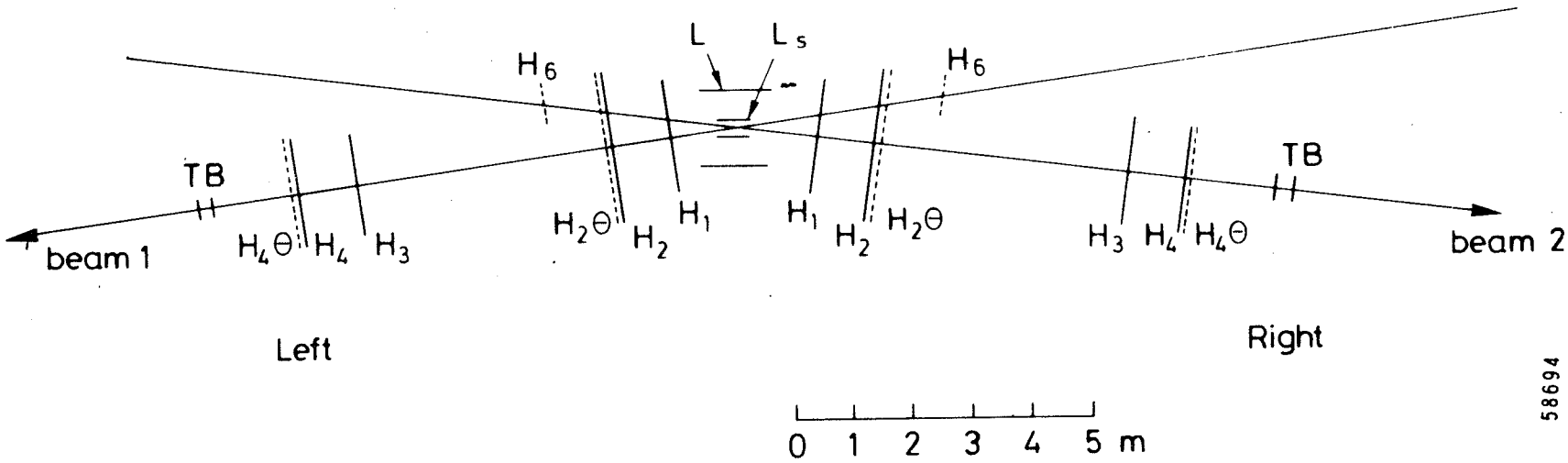

Fig. 12

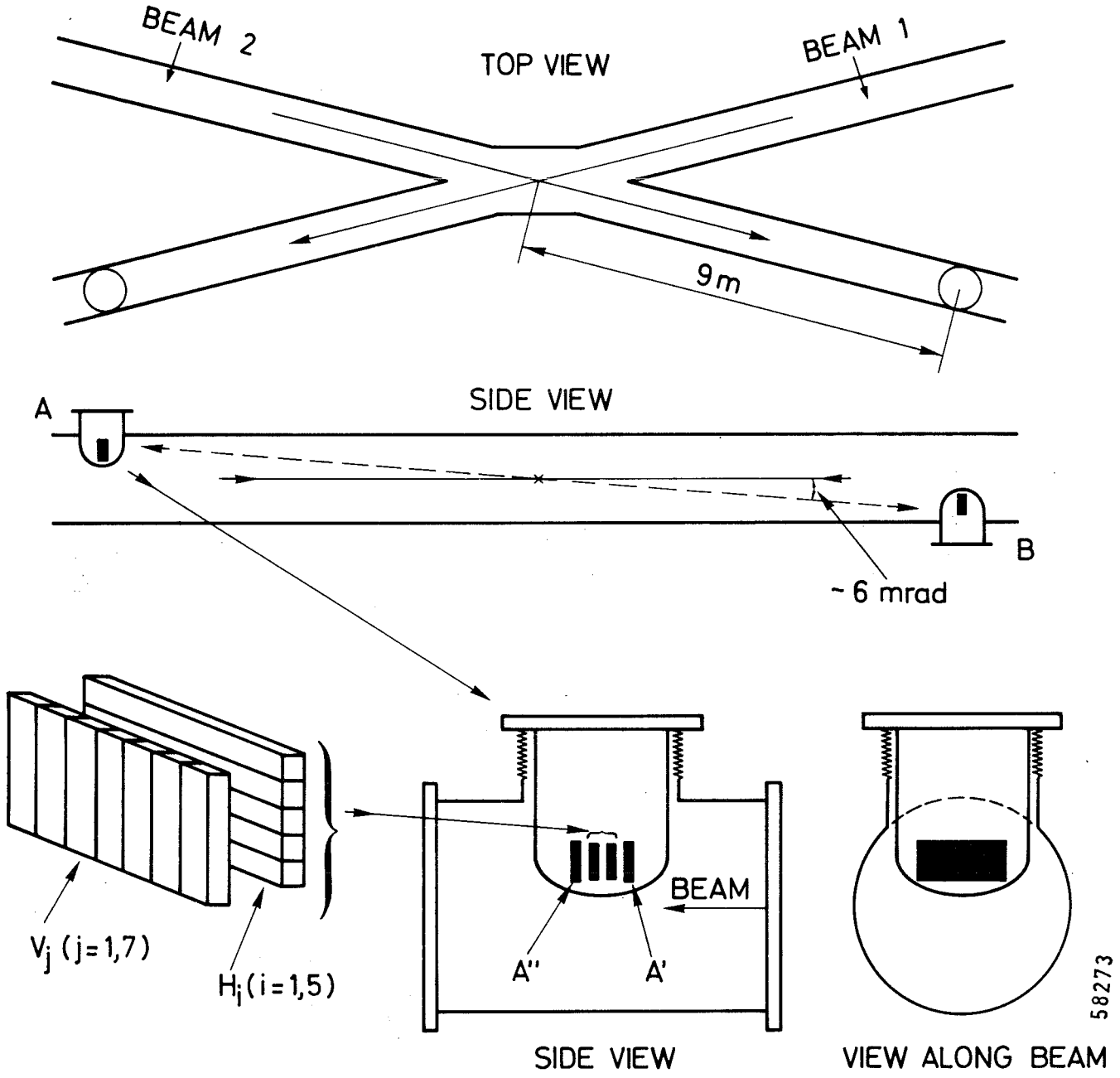
BEAM 2
TOP VIEW
BEAM 1
9m
A
SIDE VIEW
B
~ 6 mrad
V_j (j=1,7)
H_i(i=1,5)
BEAM
A''
A'
SIDE VIEW
VIEW ALONG BEAM
58273

Fig. 13

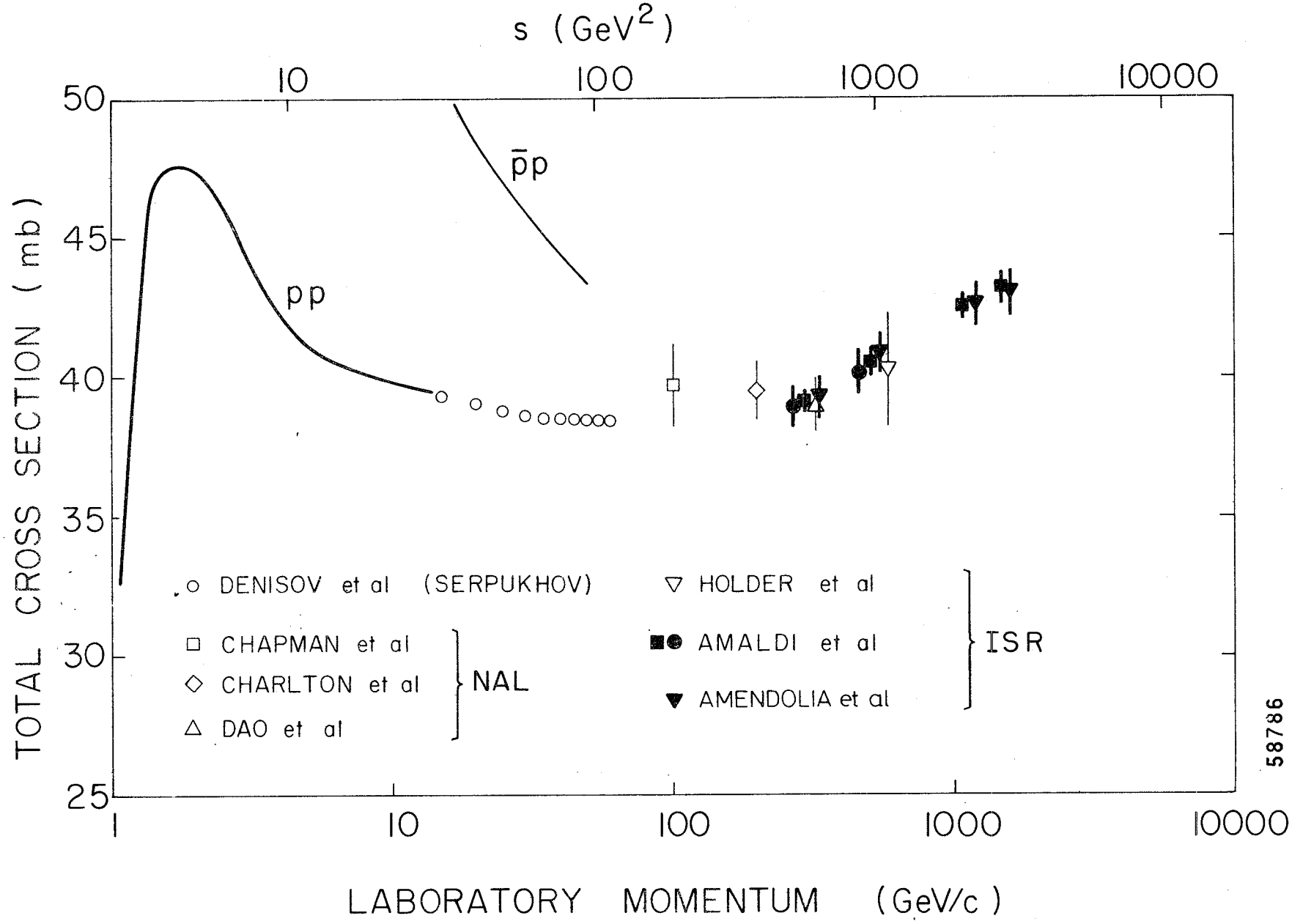
s (GeV²)
10
100
1000
10000
50
45
40
35
30
25
TOTAL CROSS SECTION (mb)
p̄p
pp
DENISOV et al (SERPUKHOV)
CHAPMAN et al
CHARLTON et al
DAO et al
NAL
HOLDER et al
AMALDI et al
AMENDOLIA et al
ISR
1
10
100
1000
10000
LABORATORY MOMENTUM (GeV/c)
58786

Fig. 14

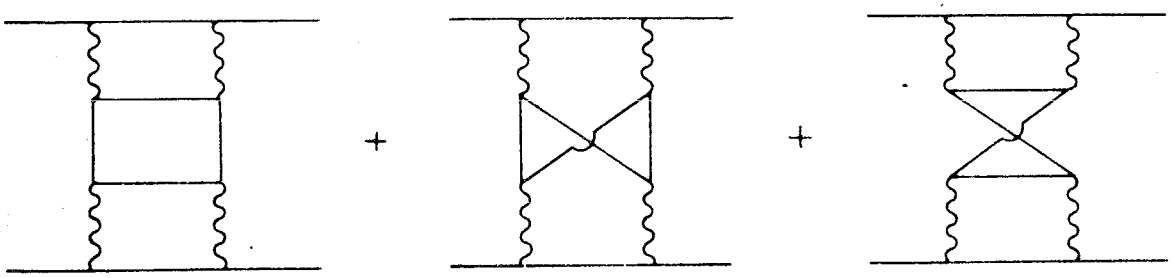

(a)

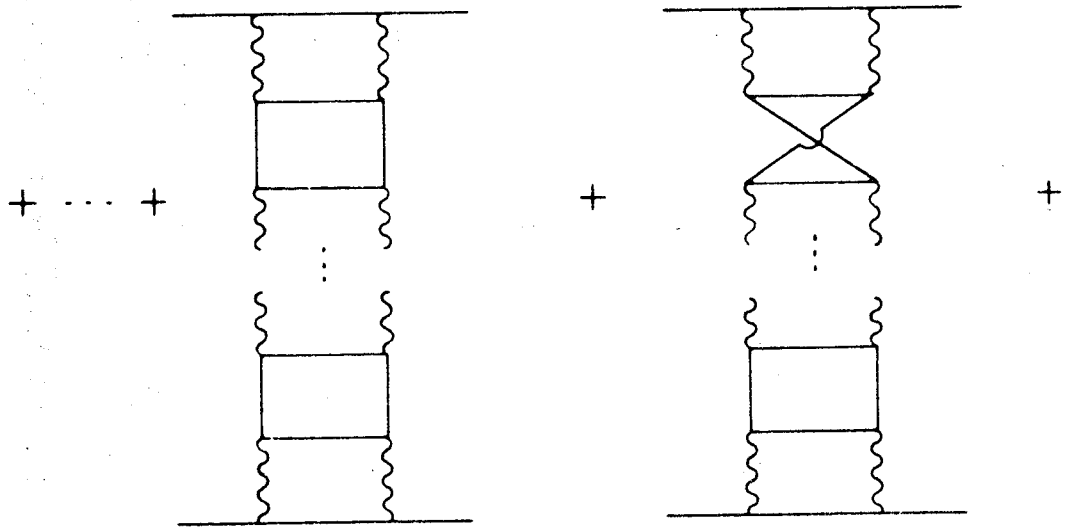

(b)

Fig. 15